

POSTGRADUATE PROGRAM DIRECTORATE

HARAMAYA UNIVERSITY

**KINETICS AND ADSORPTION POTENTIAL OF AMBO
SANDSTONE FOR THE REMOVAL OF PHOSPHATE FROM
AQUEOUS SOLUTION**

MSc THESIS

TASSEW LEMMA GURMESSA

APRIL 2019

HARAMAYA UNIVERSITY, HARAMAYA

**Kinetics and Adsorption Potential of Ambo Sandstone for the Removal of
Phosphate from Aqueous Solution**

**A thesis submitted to the Department of Chemistry, Postgraduate
Directorate**

HARAMAYA UNIVERSITY

In partial fulfillment of the requirement for the Degree of MASTER OF
SCIENCE IN CHEMISTRY

Tassew Lemma Gurmessa

APRIL 2019

Haramaya University, Haramaya

DIRECTORATE FOR POSTGRADUATE PROGRAM
HARAMAYA UNIVERSITY

As thesis research advisor, I hereby certify that I have read and evaluated this thesis prepared, under my guidance, by Tassew Lemma entitled: **Kinetics and Adsorption Potential of Ambo Sandstone for the Removal of Phosphate from Aqueous Solution**. I recommend that it to be submitted as fulfilling the thesis requirement.

Dr.Minbale Aschale
Major Advisor

Signature

Date

Dr. Endale Teju
Co-Advisor

Signature

Date

As a member of board of examiners of the MSc thesis open defense examination, I certify that I read and evaluated the thesis prepared by Tassew Lemma and examined the candidate.I recommended that the thesis be accepted as fulfilling the thesis required for degree of Master of Science in Chemistry.

Chair person

Signature

Date

Internal Examiner

Signature

Date

External Examiner

Signitue

Date

DEDICATION

This thesis manuscript is dedicated to my brother **Abera Lemma** who encouraged and strengthened me in all my life.

BIOGRAPHICAL SKETCH

The author was born in January, 1981 at Balakesa Gado, Arsii Zone, Oromia Region, Ethiopia. He attended his primary education in Habe Primary School and his secondary school in Dedea Secondary School. After completion of his secondary school education, he joined Debu University, 2003 and graduated with B.Ed. degree in Chemistry in 2006. After that, he was employed as a chemistry teacher in Yehibret Firie Senior Secondary School in Tullu Bollo Southwest Shoa Oromia Region. Then after he joined Haramaya University Directorate for Postgraduate Program in 2014 to pursue his MSc study in chemistry in summer program

ACKNOWLEDGEMENT

First of all I would like to praise the creator bestowing up on me health, strength, patience and protection throughout the study period. Secondly I would like to express my deepest gratitude to my advisors Dr. Minbale Aschale and Dr. Endale Teju for their unreserved cooperation constructive suggestions, supervision, appreciable encouragement and fatherly consultancy.

The welcome and treatment offered from the staff of chemistry of Haramaya University is sincerely acknowledged.

I would like to thank Hibret Firie Preparatory School Directors and staff for their corporation and delegation of work support. I would also like to extend my thanks to, MOE for providing me financial support to accomplish this work.

I would like to extend my gratitude to my brothers for their unreserved moral and financial support. Last but not least, my heartfelt gratitude goes to my colleagues and friends for the generous support and contribution in the accomplishment of this work

ACRONYMS AND ABBREVIATION

| | |
|-------|--|
| AS | Ambo Sandstone |
| ATP | Adenosine Tri-phosphate |
| DNA | Deoxyribo Nucleic Acid |
| RNA | Ribo Nucleic Acid |
| SEM | Scanning Electron Microscopy |
| USEPA | United State Environmental Protection Agency |
| XRD | X-ray Diffraction |
| WHO | World Health Organization |

TABLE OF CONTENTS

| | |
|--------------------------------------|------|
| DEDICATION | iii |
| STATEMENT OF THE AUTHOR | iv |
| BIOGRAPHICAL SKETCH | vi |
| ACKNOWLEDGEMENT | vii |
| ACRONYMS AND ABBREVIATION | viii |
| LIST OF TABLES | xii |
| LIST OF FIGURES | xiii |
| LIST OF TABLES IN THE APPENDIX | xiv |
| LIST OF FIGURES IN THE APPENDIX | xv |
| ABSTRACT | xvii |
| 1. INTRODUCTION | 1 |
| 1.1 Background | 1 |
| 1.2 Objectives | 3 |
| 1.2.1 General Objective | 3 |
| 1.2.2 Specific Objectives | 3 |
| 2. REVIEW LITERATURE | 4 |
| 2.1 Importance of Phosphorus | 4 |
| 2.2 Phosphate Contamination in Water | 4 |
| 2.3 Phosphorus Removal Technologies | 5 |
| 2.4 Basic Concept of Adsorption | 6 |
| 2.5 Adsorbents | 6 |
| 2.6 Adsorption Mechanism | 7 |
| 2.6.1 Chemisorption | 8 |
| 2.6.2 Physisorption | 8 |
| 2.7 Batch study | 8 |
| 2.8 Adsorption Equilibrium | 9 |
| 2.9 Adsorption Isotherm Models | 10 |
| 2.9.1 Langmuir Model | 10 |
| 2.9.2 Freundlich Model | 10 |
| 2.10 Factor that Affect Adsorption | 11 |
| 2.10.1 Adsorbent Dosage | 12 |

Table of content ('Continued')

| | |
|---|----|
| 2.10.2 Effect of pH | 12 |
| 2.10.3 Contact Time | 12 |
| 2.10.4 Initial Concentration | 13 |
| 2.10.5 Temperature | 13 |
| 2.10.6 Interfering Ions | 14 |
| 3. MATERIALS AND METHODS | 15 |
| 3.1 Description of the Ambo Sandstone Sampling Site | 15 |
| 3.2 Experimental Site | 16 |
| 3.3 Apparatus, Instruments, Chemicals and Reagents | 16 |
| 3.4 Experimental Procedure | 17 |
| 3.4.1 Characterization of the Prepared Powder Ambo Sandstone (solid-phase characterization) | 17 |
| 3.4.2 Determination of Total Phosphorus | 17 |
| 3.4.3 Batch Adsorption Experiments | 17 |
| 3.4.3.1 Effect of pH | 18 |
| 3.4.3.2 Point of Zero Charge | 18 |
| 3.4.3.3 Effect of adsorbent dose | 18 |
| 3.4.3.4 Effect of contact time | 19 |
| 3.4.3.5 Effect of agitation speed | 19 |
| 3.4.3.6 Effect of concentration | 19 |
| 3.5 Analysis of Residual Phosphate | 19 |
| 3.5.1 Determination of Adsorption Efficiency | 20 |
| 3.5.2 Analysis of Adsorption Isotherms | 20 |
| 3.6 Adsorption kinetics | 21 |
| 3.7 Adsorption thermodynamics | 22 |
| 3.8 Selectivity Interfering Ions | 22 |
| 3.9 Desorption of Phosphate | 23 |
| 3.10 Statistical Analysis | 23 |
| 4. RESULTS AND DISCUSSION | 24 |
| 4.1 Structural Characteristics | 24 |
| 4.2 Morphology Characteristics | 25 |
| 4.3 Investigation of Adsorption Parameters | 27 |
| 4.3.1 Effect of pH | 27 |

Table of content ('Continued')

| | |
|---------------------------------------|----|
| 4.3.4 Effect of Contact time | 30 |
| 4.3.5 Effect of Speed of Agitation | 31 |
| 4.3.6 Effect of Initial Concentration | 33 |
| 4.4.7 The pH Zero Point Charge | 34 |
| 4.4 Adsorption Isotherms | 36 |
| 4.4.1 Langmuir Isotherm | 37 |
| 4.4.2 Freundlich Isotherm | 38 |
| 4.5 Kinetics Studies | 39 |
| 4.6 Thermodynamics of Adsorption | 42 |
| 4.7 Interfering Ions | 44 |
| 4.8 Desorption of Phosphate | 45 |
| 5. CONCLUSIONS AND RECOMMENDATIONS | 47 |
| 5.1 Conclusion | 47 |
| 5.2 Recommendation | 48 |
| 6. REFERENCES | 49 |
| 7. APPENDIX | 57 |

LIST OF TABLES

| Table | Page |
|---|------|
| 1. The effect of particle size for adsorption process | 29 |
| 2. Initial, final and change in pH of the pH of zero point charge | 34 |
| 3. Results for phosphate adsorption isotherms | 37 |
| 4. The values of parameters and correlation coefficients of kinetic models. | 42 |
| 5. Thermodynamic parameters for phosphate adsorption onto Ambo sandstone adsorbent. | 43 |

LIST OF FIGURES

| Figure | Page |
|---|------|
| 1. Wedging sandstone beds in the Ambo quarries | |
| Error! Bookmark not defined. | |
| 2 . XRD diagram of Ambo sandstone | 24 |
| 3. SEM image of Ambo sandstone | |
| Error! Bookmark not defined. | |
| 4. The effect of pH for removal of phosphate (at initial concentration (C_0) = 30 mg/L, dose = 0.1 g, agitation speed = 120 rpm and contact time = 12 hr) | 28 |
| 5. Effect of adsorbent dose on the removal of phosphate (at initial concentration (C_0) = 30 mg/L, pH = 3, contact time = 12 hrs and agitation speed = 120 rpm) | 29 |
| 6. The effect of contact time for removal of phosphate (at initial concentration (C_0) = 30 mg/L, dose = 0.05 g, agitation speed = 120 rpm and pH = 3) | 31 |
| 7. Effect of agitation speed for removal of phosphate (at initial concentration (C_0) = 30 mg/L, pH = 3, dose = 0.05 g and contact time = 12hr) | 32 |
| 8. Effect of initial concentration for removal of phosphate [at pH = 3, dose = 0.05 g, contact time = 16 hr and agitation speed = 120 rpm] | 33 |
| 9. pH _{pzc} of the Ambo sandstone | 35 |
| 10. Langmuir (a) and Freundlich (b) adsorption isotherm of phosphate by Ambo sandstone at Ph = 3 | 37 |
| 11. Pseudo-first order (a), pseudo-second order (b) and intra-particle diffusion model (c) adsorption kinetics of phosphate by Ambo sandstone at pH = 3 | 40 |
| 12. Plot of $\ln K_c$ Vs T^{-1} for phosphate adsorption (pH = 3, dose = 0.05 g, agitation speed = 120 rpm, Contact time = 16 hr, C_0 = 50 mg/ L) | 43 |
| 13. Effect of anions on phosphate Adsorption | 44 |
| 14. Desorption of phosphate ions from Ambo sandstone using water | 46 |

LIST OF TABLES IN THE APPENDIX

| Table | Page |
|---|------|
| 1. Experimental data used to prepare calibration curve from known concentration phosphate (independent) vs spectrophotometer absorbance reading (dependent) | 58 |
| 2. Experimental data used to analyze the effect of pH on phosphate adsorption | 60 |
| 3. Batch adsorption test results analyzed to determine the effect of ambo sandstone dose on phosphate adsorption | 60 |
| 4. Batch adsorption test results analyzed to determine the effect of contact time on adsorption of phosphate by ambo sandstone | 61 |
| 5. Batch adsorption test results analyzed to determine the effect of agitation speed on adsorption of phosphate by ambo sandstone. | 61 |
| 6. Batch adsorption test results analyzed to determine the effect of initial concentration on adsorption of phosphate by ambo sandstone | 62 |
| 7. Batch adsorption test results analyzed to determine the effect of co-existing ions on adsorption of phosphate by ambo sandstone | 62 |
| 8. Batch adsorption test results analyzed for determination of phzpc on adsorption of phosphate by ambo sandstone | 63 |
| 9. Batch adsorption test results analyzed for desorption of phosphate from ambo sandstone | 63 |

LIST OF FIGURES IN THE APPENDIX

| Figure | Page |
|--|------|
| 1. Calibration Curve Prepared from Absorbance vs Concentration | 58 |

Kinetics and Adsorption Potential of Ambo Sandstone for the Removal of Phosphate from Aqueous Solution

ABSTRACT

Phosphorus plays an essential role in the development of organisms. However, phosphorus pollution known as eutrophication is regarded as one of the main causes of water quality deterioration. Therefore, the decontamination of phosphorus from aqueous solution is necessary. Thus this study was conducted to investigate the potential of Ambo sandstone as an adsorbent. Batch adsorption experiment was conducted and the following results were found. The analysis of the stone using SEM was indicated that the stone had a wide range of grain sizes from coarse, medium to fine ones. Whereas the analysis of the Ambo sandstone using XRD revealed that the stone was mainly composed of quartz (SiO₂) followed by different oxides, such as MgO, CoO and CdO. The optimum values for the studied parameters were: pH = 3, agitation speed = 120 rpm, dose = 0.05 g, contact time = 16 hr and initial phosphate concentration = 30 mg/L. Among different particle size (0.25, 0.3 and 0.75 mm) used, the smallest particle size showed the highest adsorption efficiency (86.46%). pHzpc was found to be 6.3. All the tested anions were found to interfere with phosphate adsorption, especially fluoride ion highly affect adsorption.. The desorption efficiency was small (22%) which indicates chemisorptions was involved. The Freundlich model was well fitted for experimental equilibrium data ($R^2 = 0.979$). The kinetic adsorption process was better correlate with pseudo-second-order model ($R^2 = 0.996$). The thermodynamic study parameters indicated that the adsorption process was endothermic and spontaneous. The maximum adsorption efficiency was 84.3% and the maximum adsorption capacity was 21.2 mg/g. Therefore, the sandstone is a promising adsorbent for removal of phosphate from aqueous solution.

Keywords: *Adsorption, phosphate, Ambo sandstone, wastewater, adsorption capacity*

1. INTRODUCTION

1.1 Background

Phosphorus in the form of phosphate is widely found in animals and plants (Oelker *et al.*, 2008). It is an essential element for animals and plants (Ragothama, 1999). Typically, phosphates is taken up by plants through soil and by animals through food. In addition to this, many industries use phosphorus as the main ingredient for manufacturing of chemicals such as fertilizers, detergents, paints, corrosion inhibitors, beverages and pharmaceuticals (Biswas *et al.*, 2007).

However, agricultural use of fertilizers, domestic and industrial wastewater discharge excess phosphorus in to the receiving water bodies such as natural and artificial lakes. In natural conditions, the phosphorus concentration in water is balanced with the requirement of the ecological system. But due to the factors listed above the inputs of phosphorus in to these bodies exceeds the natural conditions. This leads to increase the growth of algae (eutrophication) caused by enrichment of water by nutrients especially phosphorus, thereby inducing an undesirable disturbance to the balance of organisms in the water and to the quality of the water bodies (WHO, 2002).

Eutrophication causes algae blooms and increased growth of aquatic weeds. This in turn causes aquatic oxygen shortage as a result of decomposition of dead plants and thus loss of habitat and aquatic biodiversity (Carpenter *et al.*, 1998). Eutrophication is also the main environmental problem in Ethiopia due to the release of untreated wastewater from agricultural, industrial and domestic facilities into water bodies such as lakes (Zelalem, 2014). Generally, as eutrophication has severe impacts on the environmental and people's well being, the USEPA recommends that the acceptable level of total phosphorus in natural waters should be under 0.05 mgP/L (Mullins, 2009).

Thus, to keep the water qualities for better life there have been needed low cost and effective technologies to be developed. As a consequence, different studies have been done for removal of phosphate from wastewater started in 1950s (Biswas, 2008). A wide variety of phosphorus removal technologies have been carried out to meet the more strict

regulation. These technologies can be grouped into physical treatment (such as filtration of particulate phosphate, membrane technologies and magnetic separation), chemical treatments (such as precipitation, crystallization, anion exchange and adsorption), and biological treatment (assimilation, enhanced biological phosphorus removal and constructed wetlands (Strom, 2006). There is a general common operation principle for these technologies. First the phosphorus ions are initially changed into insoluble compounds, in the form salt precipitate or phosphorus built in microorganisms (inactivated sludge) and plant (constructed wetlands). Second the insoluble compounds are then separated from wastewater (Rybicki, 2010).

Among the methods listed above, adsorption process is generally considered to be the best water treatment option due to its convenience, ease of operation, simplicity of design and economics (Blaney *et al.*, 2007; Gupta *et al.* 2012 and Loganathan *et al.*, 2014). Currently, the adsorption process has been accomplished using different materials as adsorbent. For instance, minerals (Karageorgious *et al.*, 2007), industrial by products (Caravelli *et al.*, 2010) and soils (Gerad, 2016). Furthermore, different reports have been shown that adsorbents with high iron, alumina calcium and manganese contents have high phosphate removing efficiency Lalley *et al.*, 2016 ; Harvey and Rhue, 2008; Mustefa *et al.*, 2008). To the best of the researcher knowledge, still now there are no reports in the literature on characteristic and potential phosphate adsorption capacities of Ambo sandstone in Ethiopia. Hence, this study is used Ambo sandstone as adsorbent for removal of phosphate from aqueous solution.

1.2 Objectives

1.2.1 General Objective

The main objective of this work was to study the sorption behavior of Ambo sandstone for the removal of phosphate ions from aqueous solution.

1.2.2 Specific Objectives

- ✚ To prepare Ambo sandstone using instruments such as pestle and sieves.
- ✚ To characterize Ambo sandstone using instruments such as XRD and SEM.
- ✚ To optimize the materials with respect to some parameters: pH, adsorbent dose, contact time, size, temperature and initial concentration.
- ✚ To evaluate the adsorption process by using the Langmuir and Freundlich models.
- ✚ To evaluate the kinetics and the thermodynamics parameters for the adsorption process.
- ✚ To evaluate the desorption process.

2. REVIEW LITERATURE

2.1 Importance of Phosphorus

Phosphorus is an essential nutrient for animals and plants in the form of PO_4^{3-} and HPO_4^{2-} . Plants take phosphate from the soil through their roots and animals either by eating plants or animals. Plants use phosphorus for synthesis of ATP (adenosine tri-phosphate), DNA (deoxyribonucleic acid) and RNA (ribonucleic acid) (Barber, 2012). In animals phosphorus is the key components of teeth and bone. Additionally, phosphorus is used by many industries as a raw material. For instance, fertilizers, detergents, paints, corrosion inhibitors, beverages and pharmaceutical factories (Biswas *et al.*, 2007).

2.2 Phosphate Contamination in Water

However, due to improper management practice these industries listed above release excessive phosphorus in to water bodies around them (Paleka and Deliyanni, 2009; Xu *et al.*, 2010 and Hussain *et al.*, 2011). As a consequence, the water bodies like streams, lakes, sea and surface water become contaminated. This leads the eutrophication (extraordinary growth of algae as a result of excess nutrients release in to water bodies) which in cause by the discharge of wastewater in to water bodies like rivers, lakes and sea worldwide (Lau *et al.*, 1997 and Trepanier *et al.*, 2002). Because of these algae blooms and depletion of oxygen will occur in water bodies (Hub, 2013).

Growth of phytoplankton, algae and macro plants rapidly accelerate when the concentration of phosphorus in aquatic system is high. When they die, large amount of oxygen is used for decomposition their dead bodies. As a result the amounts of dissolved oxygen become diminished than uncontaminated water contain. As a consequence, the aquatic plant and animals affected due to lack of oxygen (Biswas, 2008; Benyousef and Amrani, 2011). In addition, there are also many other adverse effects. For instance, the aquatic plants are declined and the dead zone is formed. As a result, the whole ecosystems become severe from disappearance. Not only this can the people's health be negatively affected due to the consumption of poisonous fish and shellfish in eutrophication regions

.Consequently, these people severe from skin irritation, gastrointestinal illness, neurological damage and death. This indicates that eutrophication has adverse effect on human well being and the environments are highly affected. In response to this the USEPA recommended that the acceptable level of total phosphorus in natural waters should be under 0.05 mgP/L (Mullins, 2009).

2.3 Phosphorus Removal Technologies

Due to the problem described under section 2.1, before discharging wastewater in to water bodies removing phosphate is usually obligatory. Because of this wastewater treatment has been developed. Concerning this the need to reduce the excess phosphate entering water bodies started late 1950s. Then afterward different techniques have implemented for the removal of phosphorus from wastewater, even though in many cases it is performed and leads to major contamination on a wide world level. The wastewater treatment industry presently uses several techniques to remove phosphorus (Duenas *et al.*, 2003). Some are used large scale treatment facilities and some are only experimental projects and others still on small-scale basis (Van Loosdrecht *et al.*, 1997 and Stratful *et al.*, 1999). In all cases phosphorus is removed by converting the phosphate ion in wastewater into solid fractions. Among the common removal technologies are: ion exchange (Ghafari *et al.*, 2008), reverse osmosis (Shrimalias, 2001), electrodialysis (Bernardes, 2014), bioremediation (Akpore and Muchie, 2010) and Chemical precipitation (Nassef, 2012) are commonly used. These techniques have their own merits and demerits in using wastewater treatment. A short description of the advantages and disadvantages of these techniques are explained below.

One of the benefits from using chemical precipitation is that it is sufficiently applicable for high phosphate concentration (Tillontson, 2006). Nevertheless, due its high chemical amount, high cost and storage problem its use becomes limited. These factors in turn affect subsequent biotreatment.

Biological treatment is also commonly applied due to relatively high removal rates. However, they require complex and expensive cycling systems to remove the aerobic

effluent (Hesselmann *et al.*, 2000). On the other hand, the significant drawbacks of reverse osmosis and electrodialysis are due to lack of inefficient removal performance and high cost (Rodrigues and Silva, 2009). Ion-exchange is also among the common wastewater treatment techniques currently used. One of the advantages for using crystallization techniques for wastewater treatment is its final product can be used as fertilizers. But its increased salinity and its complexity of operating system limit its usage (De-Bashan and Bashan, 2004). Among the techniques described above adsorption is preferable for treatment of wastewater. This is due to its low sludge production, easy operation; high rate, superior selectivity and more rapid regeneration process (Yang *et al.*, 2014).

2.4 Basic Concept of Adsorption

Adsorption is an accumulation or enrichment of chemical substance onto a surface or interface. The adsorbing phase is defined as the adsorbent and the material being adsorbed is adsorbate. The adsorbent is required to have an extremely large surface area on which the adhesion of contaminant can occur. Phases on which adsorption takes place can be between gas-liquid, liquid-liquid or liquid-solid (Worch, 2012). Since adsorption is a surface based process, the surface area plays an important role in deterring adsorbents' quality. In addition to this solids should have active and energetic sites which are able to interact with solute due to their specific electronic and spatial properties (Crittenden *et al.*, 1998).

2.5 Adsorbents

Adsorbents are the solid materials whose surfaces are used for the accumulation of the desired compounds and they play important roles in the extent of adsorption processes. Activated carbon, silica gel, MCM-41, MCM-48, activated alumina, zeolites and molecular sieves, carbon nanotubes, pillared clays, polymeric resins have been widely applied in gas – bulk separation, gas purification, and liquid – bulk separation and liquid purification due to their superior characteristics (Yang, 2003). The performance of an adsorbent is dependent on the solid's performance in equilibrium and kinetics. High

adsorption capacity is an asset; however, if the contact time is too long, the efficiency of the adsorbent reduces. Same way, a rapid adsorption with low capacity is also undesired. Therefore, optimum solids fulfilling these criteria should be chosen in order to meet these needs (Do, 2008).

- ✚ The adsorbent should comprise high surface area or micropore volume.
- ✚ The adsorbent must have large pore network for molecule transformation into the inner layers. IUPAC classified the pores and the structure of the sorbent according to the pore diameter as follows (Do, 2008):

Micropores $d < 2 \text{ nm}$

Mesopores $2 \text{ nm} < d < 50 \text{ nm}$

Macropores $d > 50 \text{ nm}$).

A favorable adsorbent is also expected to exhibit following characteristics: high energy density, high energy efficiency, high adsorption capacity, high adsorbent-adsorbate affinity, satisfactory potential for regeneration, ease of operation, cost-efficiency, low desorption temperature, low toxicity and low environmental impacts (Lefebvre and Tezel, 2017 and Tholiso *et al.*, 2017).

2.6 Adsorption Mechanism

Four main steps of adsorption process can be summarized as follow (Soletto *et al.*, 2013).

- ✚ Solute is transferred from the liquid to the adsorbent's boundary layer.
- ✚ External diffusion occurs thus the solute is transferred to the surface of the adsorbent through the boundary layer.
- ✚ The solute is diffused from the surface to active sites, termed intra-particle diffusion.
- ✚ Sorption of the adsorbate to the solid phase, by several forces described below.

In most cases, two primary driving forces lead to the adsorption a solute from the aqueous media .The first driving force is linked with the solvent disliking (lyphobic) character of the solute. A hydrophobic substance tends to adsorbed while a hydrophilic substance tends to stay in aqueous media. The solubility of the adsorbed substance is

essential in determining the intensity of the adsorption process. The second driving force is the electrical attraction of the solute to the solid. This type occurs as a result of chemical interaction or Van der Waals attraction with the adsorbent. The adsorption induced by Van der Waals force is defined as physisorption and chemical interaction is termed as chemisorptions. In the adsorption process, these two types interact together and it is quite difficult to differentiate between the two (Cecen and Aktas, 2012 and Worch, 2012).

2.6.1 Chemisorption

In chemisorption, electrons in specific surface sites and solute molecules are exchanged, resulting in the formation of a strong chemical bond. Chemically adsorbed adsorbates are immobilized within the surface or on the surface. Since chemical reaction happens more rapidly at high temperature. This means that chemisorptions are more predominant at high temperature compared to physisorption. It has high adsorption enthalpy (40-800 KJ/mol) (Cecen and Aktas, 2012).

2.6.2 Physisorption

In physisorption, intermolecular attractions occur between favorable energy sites. The adsorbate is attracted to the surface by weak Van der Waals forces in physisorption. Hence it is less strongly attached to the surface compared to chemisorptions. There is not any exchange of electrons in this process. In contrast to chemisorptions, occurs at low temperature and need less enthalpy (5-40 KJ/mol) (Cecen and Aktas, 2012). For the wastewater treatment techniques like adsorption in addition to the adsorption mechanism selection of type of adsorbent (material) is an essential criteria. Commonly natural, commercial and synthetic materials are used for adsorption process. Some of the adsorbing materials are described below.

2.7 Batch study

In batch contact unit systems, a predetermined amount of adsorbent is mixed with the water for a given contact period and subsequently is separated by sedimentation or

filtration. The flexibility of this process makes it adaptable for many applications particularly in drinking water treatment plants. The adsorption process is characterized by mainly two phenomena: adsorption equilibrium,

2.8 Adsorption Equilibrium

Adsorption equilibrium is described by an equation relating the amount of adsorbate adsorbed onto the adsorbent and the equilibrium concentration of the adsorbate in solution at a given constant temperature (Chaudhary *et al.*, 2003 and Sincero, 2003). The analytical forms of adsorption isotherms are complex due to the solid surfaces' structural and energetic heterogeneity. As the adsorption processes proceeds, the adsorbed adsorbate tend to desorb into the solution until the rates of adsorption and desorption attain an equilibrium state which is called adsorption equilibrium. At equilibrium, no change can be observed in the concentration of the adsorbate on the solid surface or in the bulk solution. The position of equilibrium is characteristic of the entire system, the adsorbate, adsorbent, solvent, temperature, pH, and so on.

Adsorbed quantities at equilibrium usually increase with an increase in the adsorbate concentration. The presentation of the amount of adsorbate adsorbed per unit mass of adsorbent as a function of the equilibrium concentration in bulk solution, at constant temperature, is termed the adsorption isotherm. Equilibrium adsorption is the most informative and important test for estimating the adsorption capacity of an adsorbent for an adsorbate in a given condition (concentration and temperature) and the competition among adsorbates in the case of multi-component adsorption (Suzuki, 1990). Description of adsorption equilibrium by an appropriate isotherm equation is the first step in the design of an adsorption system since it reflects the capacity or affinity of an adsorbent for a particular adsorbate. At the end of the equilibrium period the aqueous phase concentration of the adsorbate is measured and the adsorption equilibrium capacity is calculated for each experiment using the mass balance expression,

$$q_e = \frac{(C_o - C_e)}{M} \times V \quad (1)$$

$$\text{Removal efficiency (\%)} = \frac{(C_0 - C_e)}{C_0} \times 100 \quad (2)$$

where, q_e = equilibrium adsorbent-phase concentration of adsorbate, mg adsorbate/g adsorbent; C_0 = initial aqueous-phase concentration of adsorbate, mg/L; C_e = equilibrium aqueous-phase concentration of adsorbate, mg/L; V = volume of the solution (L) and M = mass of adsorbent (g). Removal efficiency is calculated using equation 2.

2.9 Adsorption Isotherm Models

2.9.1 Langmuir Model

At equilibrium, the Langmuir equation represents the maximum capacity of the adsorbent $q_e = \frac{q_{max}K_L C_e}{1 + K_L C_e}$. And a simple modification leads to equation 4 which is the equation for the Langmuir adsorption isotherm model,

$$q_e = \frac{q_{max}K_L C_e}{1 + K_L C_e} \quad (3)$$

Where, C_e = equilibrium concentration of the adsorbate (mg/L), q_e = amount of the adsorbate adsorbed per unit mass of the adsorbent (mg/g), q_{max} = maximum amount of the adsorbate adsorbed per unit weight of the adsorbent (mg/g); K_L = Langmuir constant related to the energy of adsorption (L/mg). The Langmuir isotherm model advocates that uptake occurs on a homogeneous surface by monolayer adsorption without adsorbed molecules interacting. The model assumes uniform energies of adsorption onto the surface and no transmigration of adsorbate in the plane of the surface (Hameed *et al.*, 2007). This model can be linearised as follows:

$$\frac{C_e}{q_e} = \frac{1}{q_{max}K_L} + \frac{C_e}{q_{max}} \quad (4)$$

2.9.2 Freundlich Model

Unlike the Langmuir isotherm, the Freundlich isotherm is an empirical model which does not imply a maximum adsorption capacity of the adsorbent (Amuda and Ibrahim, 2006).

In the Freundlich equation the adsorbed amount increases infinitely with the increase in concentration, which is unrealistic. The Freundlich adsorption equation is perhaps the most widely used mathematical description of adsorption in aqueous systems. The Freundlich equation is expressed as follows (Freundlich, 1926):

$$q_e = K_L (C_e)^{\frac{1}{n}} \quad (5)$$

This model can be linearised as follows:

$$\ln q_e = \ln k_f + \frac{1}{n} \ln C_e \quad (6)$$

where, C_e = equilibrium concentration of adsorbate (mg/L), q_e = amount of adsorbate adsorbed per unit mass of adsorbent (mg/g), K_f and n = Freundlich constants (mg/g). K_f (mg /g) (L/mg) $1/n$ and n (dimensionless) are the Freundlich constants determined from the linear regression analysis. The value of the parameter n is representative of both the adsorption intensity and the surface heterogeneity. Despite the fact that parameter n lacks physical meaning, it is generally admitted that $0 < 1/n < 1$ indicates favorable adsorption, while $1/n = 1$ characterizes a linear adsorption phenomenon (Fytianos *et al.*, 2000). The K_f constant may be considered as a rough indication of the adsorption capacity expressed or as an adsorption affinity parameter. The Freundlich isotherm's drawback is that it does not converge with Henry's law at low surface coverage. Therefore it fails to describe equilibria as $q \rightarrow 0$ and is thermodynamically inconsistent (McKay, 1996). However, this problem has been overcome by extrapolation of data to zero concentration (Fritz and Schlunder, 1981) and its ability to fit a broad set of experimental data still makes it a popular model for studying adsorption and ion exchange phenomena.

2.10 Factor that Affect Adsorption

Adsorption is not a homogeneous process and a variety of factors affect its efficiency. Besides physical properties of the adsorbent such as porosity, internal surface area, and external surface area, wastewater's properties also have significant influences on the

overall removal efficiency. The most important characteristics of the feed solution and the adsorbents are reviewed below.

2.10.1 Adsorbent Dosage

All scientific studies indicated that phosphorus adsorption increased with increasing adsorbent dose up to a specific level, and then it remained constant. One simple explanation for this is that by adding more adsorbent to the solution, more binding sites are available for the sorption process. Thus, high amounts of phosphate ions can be adsorbed. In most studies, the range of adsorbent dosage is between 0.5 and 2 g/L for 250 mL wastewater (Kumar *et al.*, 2010).

2.10.2 Effect of pH

The effect of pH is considered in the adsorption process because it may affect both the properties of the adsorbent and the composition of the solution. It is also important due to the ionization of surface functional groups and composition of solutions (Chelangat *et al.*, 2015). For negatively adsorbates usually high adsorption is occurred at lower pH, due to the columbic interaction between adsorbent and adsorbates. Whereas at higher pH the adsorption of adsorbates decreases, due the columbic repulsion between the surface of adsorbents and adsorbates.

2.10.3 Contact Time

The adsorption process in aqueous solution is affected by contact time. In the beginning, there is large number of vacant sites in the adsorbents and adsorbates are adsorbed instantaneously onto these binding sites. This instantaneous sorption of adsorbates could be the result of specific chemical interaction or other driving forces like diffusion. Then there is slow uptake of adsorbates where all the active sites over the adsorbent surface are utilized before saturation. The fall in adsorption rate is because of the relocation of adsorbate ions from boundary layer to the interior porous surfaces. So, transportation rate of the ions from exterior to interior sorption sites determines the rate of adsorption in following phases. Later on, the binding sites became limited and remaining sites were not

occupied because of the repulsive forces between adsorbates on solid surface and the bulk phase. Finally, adsorbates removal rate leveled off significantly, which denotes the equilibrium phase (Poudyal, 2015).

2.10.4 Initial Concentration

Generally, the adsorption efficiency decreases if there is a significant increase in the initial concentration of phosphate. The percentage adsorption of phosphate onto iron hydroxide eggshell decreased from 95% to 64% when initial phosphate concentration increased from 2.8 mg/L to 110 mg/L (Mezenner and Bensmaili, 2009). However, in another study by Xu *et al.* (2009), they observed an increase in phosphate uptake capacity when the initial concentration was raised from 100 mg/L to 300 mg/L.

2.10.5 Temperature

Adsorption is affected by the relations between the properties of the adsorbent and the solute. Thus, the effects of temperature are different for different adsorbents and solutes. In general, numerous studies have shown that by increasing the temperature of the solution to a specific range, the adsorption efficiency of different adsorbents also increases. Saha *et al.*, (2010) found that at pH = 3, the maximum amount of phosphate adsorbed per gram of added granular ferric hydroxide occurred at 45 °C. Mezenner and Bensmaili (2009) showed that the phosphorus adsorption capacity of iron hydroxide eggshell increased as the solution was heated from 20 to 45 °C. Benyoucef and Amrani (2011) attributed the higher phosphorus adsorption capability with increasing temperature to the expansion of pore size at higher temperatures. Moreover Kumar *et al.* (2010) suggested that elevated temperature leads to an increase in the rate of diffusion of phosphate ions, which in turn enhances the adsorption efficiency. However, it is important to note that higher temperature is not always beneficial for the process. In a study conducted by Yue *et al.* (2010), there was a decrease in the phosphorous sorption capacity of modified giant reed as the temperature increased from 30 to 60 °C. The researchers proposed that desorption of phosphate ions from the adsorbent surface might be accelerated at this temperature range.

2.10.6 Interfering Ions

Since wastewater contains various anions, which may interfere in the process, many researchers have studied their potential effects on the adsorption efficiency. Divya *et al.* (2012) stated that the presence of anions like Cl^- , SO_4^{2-} , NO_3^- and CO_3^{2-} did not show any significant influence on phosphate adsorption, whilst some cations such as Ca^{2+} , Mg^{2+} , Cu^{2+} , Fe^{2+} and Zn^{2+} facilitate the process. These findings coincide with those reported by Chen *et al.* (2014). They concluded that anions of Cl^- , NO_3^- and SO_4^{2-} had a negligible effect on phosphorus adsorption by natural pyrite. On the other hand, a study conducted by Zhang *et al.* (2012) showed that SO_4^{2-} and CO_3^{2-} had a negative influence on the phosphate uptake of lanthanum-doped activated carbon fiber. These results demonstrated the complex nature of adsorption process, especially when competing ions are involved.

3. MATERIALS AND METHODS

3.1 Description of the Ambo Sandstone Sampling Site

Ambo sandstone for the adsorption study was collected from Ambo district of Senkele mineralogy site which is located about 125 km west of Addis Ababa city. Senkele district is a small just 4 km to southwest of Ambo town. Here hora water was used by livestock for drinking purpose for a long time ago. The Ambo sandstone is mostly used for the building purpose. Regarding building stone, the best potential of sandstone lies within the thick, red bed series of the Adigrat Sandstone along an axis from Ambo in the south, through the Abay valleys to Tigray in the north. Exploitation mainly occurs in the deposits near the town of Ambo (Figure 1). Here, the cross-bedded, red and white sandstone is worked to ashlars, split bricks and slabs mainly with the help of simple tools such as sledge hammers, wedges and crow bars (Heldal *et al.*, 1997). Products are distributed throughout most of Ethiopia, even though a major part of the production is used in the capital.



Figure 1. Wedging sandstone beds in the Ambo quarries.

3.2 Experimental Site

For preparation of Ambo sandstone, the sandstone was brought to Haramaya University staff lab and washed with water to remove dirt particles. It was then dried, crushed and milled into smaller sizes using mortar and pestle. The crushed Ambo sandstone was sieved through sieves to obtain the desired particle size range (0.25 mm, 0.3 mm, and 0.75 mm). Finally, they were categorized according to the particle size and sealed in bottles. XRD characterization of the prepared adsorbent was done at Addis Ababa University. Scanning electron microscopic study was conducted at Addis Ababa Science and Technology University.

3.3 Apparatus, Instruments, Chemicals and Reagents

The laboratory apparatus that were used during the study included different sized glassware (beaker, volumetric and Erlenmeyer flasks, cylinders, pipettes, dropper and funnels filter paper, mortar and pestle and different sieves (0.25 mm, ASTM E11, 0.30 mm, Madison filter and 0.75 mm). The instrument used in this study were pH meter (MP 220), XRD (BRUKER D8 Advanced XRD), UV-Vis spectrophotometer (SANYO, SP65), rotary shaker (orbital shaker SO1 made in UK), electronic balance (OHAUS, made in Switzer Land) and scanning electron microscope (SEM).

Standard solutions of phosphate were prepared from dihydrogen potassium phosphate, (KH_2PO_4) (99% BDH– Chemical Ltd poole England). Ammonium molybdate, ($\text{Mo}_7\text{O}_{24}\cdot 6(\text{NH}_4)\cdot 4(\text{H}_2\text{O})$), (Nice chemicals pvt.ltd COCHIN, 98%), tin (II) chloride 2-hydrate, $\text{SnCl}_2\cdot 2\text{H}_2\text{O}$ (BDH-GPR), sulpheric acid (H_2SO_4) (Lobal chemie. laboratory reagent and fine chemicals) were used for Uv-Visible analysis of phosphate; pH of the solutions was adjusted by using NaOH and HCl.

3.4 Experimental Procedure

3.4.1 Characterization of the Prepared Powder Ambo Sandstone (Solid-phase characterization)

X-ray diffraction (XRD) analysis of the powder Ambo sandstone was made by Bruker D₈ advanced XRD equipped with Cu-K_{a1} radiation ($\lambda = 0.154$ nm) at a scanning speed of 10⁰/min ranging from 10° to 60° operated at a voltage of 40 kV and applied potential current of 15 mv. The the raw data resulted from XRD were analyzed and interpreted by match software. The scanning electron microscope (SEM) is one of the most used characterization techniques applied for studying the surface morphology, properties, porosity and texture morphology of adsorbent. SEM analysis was carried out at room temperature with accelerating voltage of 10 kV and 5.00 kV

3.4.2 Determination of Total Phosphorus

25 g of (NH₄)₆Mo₇O₂₄ · 4H₂O was dissolved in 175 mL of distilled water. Cautiously 280 mL of conc. H₂SO₄ was added to 400 mL distilled water. Then after cooling, molbdate solution was added to H₂SO₄ solution and diluted to 1 L. 2.5 g of fresh SnCl₂·2H₂O was dissolved in 100 mL glycerol. Then it was heated in a water bath by stirring with a glass rod to hasten dissolution. Those reagents were placed in a refrigerator before used for analysis. Then they were used for determination of phosphate spectrophotometrically by stannous chloride method (APHA, 1998).

3.4.3 Batch Adsorption Experiments

All adsorption studies were carried out in Erlenmeyer flaks of 50 mL having an adsorbent ratio of 1 : 50 (0.05 g of sandstone powder : 25 mL of 30 mg/L of KH₂PO₄ reacting solution) after the dose was optimized. The pH of phosphate solution was adjusted using dilute HCl and NaOH solutions by using pH meter. Equilibration for sorption experiments were done on a rotary shaker. After the contact duration, the suspensions were withdrawn, filtered through Whatman filter paper and analyzed for residual phosphate concentration by (UV-Visible) spectrometer using stannous chloride method (APHA,

1998). The difference between the initial and the final concentration was considered as the amount of phosphate adsorbed and retained by the sandstone. The optimum parameters for adsorption including dose of Ambo sandstone, particle size, contact duration, pH and initial phosphate concentration were investigated through batch adsorption tests.

3.4.3.1 Effect of pH

To identify the influence of pH on the phosphate adsorption, experiments were carried out by adding 0.1 g of the adsorbent into 50 mL Erlenmeyer flask containing 25 mL of 30 mg/L phosphate ions (anhydrous KH_2PO_4 was used to prepare a 1000 mg/L phosphate ions stock solution) and by varying pH of the solutions from 2, 3, 4, 7 and 9. Adsorption experiments were carried out while keeping other parameters constant (agitation speed at 120 rpm, contact time at 12 h and initial phosphate ions concentration at 30 mg/L). Each time the pH of the solutions was adjusted with dilute HCl or/and NaOH solution. Then equilibrium phosphate ion concentration was measured after the solutions were agitated for 12 hr.

3.4.3.2 Point of Zero Charge

The pHPzc of the Ambo sandstone was determined by adding 0.05 g of Ambo sandstone in 50 mL beaker. 25 mL of 0.001 M NaNO_3 was added and the pH was adjusted by using dilute HCl or NaOH ranging from 2 to 9. The solution was equilibrated for 1 hr in a mechanical shaker and the initial pH was determined. Then 1 g of NaNO_3 was added to the above solution and further equilibrated for another 1 hr. After agitation the final pH was determined. A plot of pH final –initial (y-axis) versus pH final (x-axis) was used to determine the point of zero point charge where the graph intersects the x-axis.

3.4.3.3 Effect of adsorbent dose

For determining of the effect of adsorbent dose of phosphate adsorption, the amounts of phosphate ions adsorbed were determined by varying the dose as 0.01, 0.05, 0.075,

0.1, 0.5 and 1 g with initial phosphate ions concentration, agitation speed and contact time kept constant, and the pH value kept at the optimized value.

3.4.3.4 Effect of contact time

For determining of the effect of contact time of phosphate ions adsorption, the amounts of phosphate ions adsorbed were determined by varying the contact time as, 3, 6, 12, 16 and 24 h. With pH and adsorbent dose being kept at the optimized values whereas the agitation speed and initial phosphate concentration were kept constant.

3.4.3.5 Effect of agitation speed

To study the effect of agitation speed of phosphate ions adsorption, the quantity of phosphate ions adsorbed were determined by varying the agitation speed as, 50, 100, 120, 140 and 160 rpm with pH, adsorbent dose and contact time kept at optimized value, whereas initial phosphate concentration was kept constant.

3.4.3.6 Effect of initial concentration

To study the effect of initial adsorbate concentration, the experiment was carried out using different initial phosphate ions concentrations (10, 20, 30, 50 and 60 mg/L). 0.05 g of the adsorbent was loaded into a 50 mL Erlenmeyer flask and 25 mL of each of initial phosphate ions solution was then added. Each time the pH of the solution was maintained at the optimized value by manually adding 0.1 M HCl or 0.1 M NaOH solutions. The flask was capped and shakes on rotator shaker at 210 rpm for 16 h to ensure approximate equilibrium. At the end of the adsorption period, the solution was filtered and then analyzed for phosphate ions equilibrium concentration.

3.5 Analysis of Residual Phosphate

For each of the batch adsorption test after the contact duration period, the resulting suspensions were filtered using a filter paper and the filtrate was analyzed for the residual phosphate concentration through Stannous Chloride method (APHA, 1998). The method utilizes a stannous chloride reduction where by the phosphate reacts with ammonium

molybdate and is then reduced by stannous chloride to form a blue complex. The extent of absorbance of the blue coloring was measured by using 67 UV/Vis Spectrophotometer and the respective residual phosphate concentration were calculated from the spectrophotometry reading value via the formula established by calibration curve (Appendix 1).

3.5.1 Determination of Adsorption Efficiency

The Ambo sandstone phosphate adsorption efficiency, following each batch adsorption test, ultimately calculated using the equation given below (Vanderborght and Griekenm, 1977)

$$\text{Adsorption (\%)} = \frac{C_o - C_f}{C_o} \times 100 \quad (7)$$

Where:

C_o = initial phosphate (PO_4^{3-}) concentration (mg/L)

C_f = final phosphate (PO_4^{3-}) concentration (mg/L)

3.5.2 Analysis of Adsorption Isotherms

The adsorption capacity of the Ambo sandstone is the mass of phosphate adsorbed on the Ambo sandstone (adsorbent), and was calculated based on the mass balance principle and formulae Vanderborght and Van Griekenm (1977) as described below:

$$q_e = \frac{C_o - C_e}{M} \times V \quad (8)$$

Where q_e = adsorption capacity of the Ambo sandstone (mg/g)

V = the volume of reaction mixture (L)

M = the mass of adsorbent used (g)

C_o = the initial phosphate concentration (mg/L)

C_e = the residual or equilibrium phosphate concentration (mg/L)

The affinity of the adsorbate for an adsorbent is quantified using adsorption isotherms. For this purpose both Freundlich and Langmuir models were employed to describe the

experimental results of phosphate ions adsorption, by keeping all parameters at optimized conditions. Initial phosphate concentration was varied from 10 to 60 mg/L. In separate flask 25 mL of solutions containing different amounts of initial phosphate ions concentration were added. After the reaction period, all samples were filtered and analyzed for the corresponding phosphate ion concentration. Those experimental results were used for Langmuir model and Freundlich model according to the following formulas respectively.

$$\frac{C_e}{q_e} = \frac{1}{q_m b} + \frac{1}{q_m} C_e \text{ and } \log q_e = \frac{1}{n} \log C_e + \log k \quad (9)$$

Where:

C_e is the equilibrium adsorbate concentration in the solution.

q_e is the equilibrium adsorbate uptake on the adsorbent (mg/g)

q_m is the maximum adsorption capacity (mg/g)

b is the Langmuir constant that is related to the affinity of binding sites and related to the energy of sorption (L/mg)

n and k are Freundlich constants related to adsorption intensity and adsorption Capacity respectively.

3.6 Adsorption kinetics

Adsorption kinetics modules were carried out in order to determine the contact time required to reach the equilibrium. 25 mL samples and 30 mg/l phosphate solutions were mixed with 0.05 g of sandstone powder particle size 0.250 mm constant temperature 25 °C by varying the time from 3, 6, 12, 16 and 24 h. Pseudo-first-order model and pseudo-second order model were studied. The above process and the experimental results pseudo-first-order model and pseudo-second-order model were tested using the following formula respectively.

$$\ln(q_e - q_t) = \ln q_t - k_1 t \text{ and } \frac{t}{q} = \frac{1}{k_2 q_e^2} + \frac{t}{q_e} \quad (10)$$

Where:

q_e is the amount of adsorbate adsorbed (mg/g) at equilibrium,
 q_t is the amount adsorbate adsorbed (mg/g) at a time t ,
 k_1 is the pseudo-first –order adsorption rate constant (L/t) and
 k_2 is pseudo-second-order rate constant (L/t).

In addition to pseudo-first order and pseudo-second order, the intra-particle diffusion model was also tested based on the following formula.

$$q_t = a + k_{int}t^{0.5} \quad (11)$$

Where

k_{int} is the intra-particle diffusion rate constant (mg/g min) and a is an intercept which gives an idea about the thickness of the boundary layer.

3.7 Adsorption thermodynamics

Adsorption thermodynamics were studied at the same condition of the adsorption isotherms study to determine the thermodynamic parameters enthalpy change (ΔH°), entropy (ΔS°) and free energy change (ΔG°).

3.8 Selectivity Interfering Ions

The selectivity of phosphate adsorption experiment was done according to the method described by Seiki *et al.* 2003). To determine the effect of common existing anions on the adsorption of phosphate by Ambo sandstone, 30 mg/L of each was prepared from sodium fluoride, sodium chloride, sodium sulfate, and sodium hydrogen carbonate including dihydrogen phosphate. Equal volume of phosphate and each ion were mixed together and filled with distilled water to 25 mL. The solution pH was adjusted to 3. The solutions were agitated at 120 rpm for 16 h. After filtration, the residual concentration of phosphate was analyzed. Then the effect of common coexisting ions such as: fluorides, chloride, sulfate, and carbonate on the adsorption of phosphate were investigated.

3.9 Desorption of Phosphate

Phosphates ions desorption were studied using phosphate ions loaded powder samples. 0.05 g of Ambo sandstone of phosphate loaded powder was added into each flask containing 25 mL of distilled water. 0.1 M NaOH and 0.1 M HCl solutions were used to adjust pH of the solution from 2, 3, 4, 7, and 9. The solutions were agitated at optimized value (120 rpm). The filtrate was analyzed for phosphate ions according to the method described previously. The quantity of desorbed phosphate ions was determined by the amount of phosphate ions in the solution after each desorption experiment was performed.

3.10 Statistical Analysis

The various adsorption tests were conducted in triplicate, and statistical analysis of all data was performed with MS Excel.

4. RESULTS AND DISCUSSION

4.1 Structural Characteristics

The XRD pattern of the Ambo sandstone test is presented in Figure 2. The XRD analysis revealed that Ambo sandstone primarily composed of quartz with less amount of feldspar and clay phases. Similar results were reported for analysis of Newcastle sandstone(Jones *et al.*, 2013). It was observed that the strongest peak at $2\theta = 26.86^\circ$ could be assigned to quartz and different silicon oxide phases. Those oxide phases were identified using matchsoftware analysis. Whereas other peaks which appeared to the left and right of the main peak indicated a mixture of different phases. Among them the common oxide nphases are MgO, CoO and CdO . However some literature reports show that similar sandstone mainly composed of Si and O followed by Mg, Al, Ca ,Ti , Fe etc. (Mounia et at., 2013). Anyhow, these peaks indicated the crystalline structure of Ambo sandstone. Generally the main peak indicated the highly organized crystalline structure of the powder and the smaller peaks which are the secondary ones revealed that the less organized crystalline structure of the powder Ambo sandstone (Rahab *et al.*, 2016).

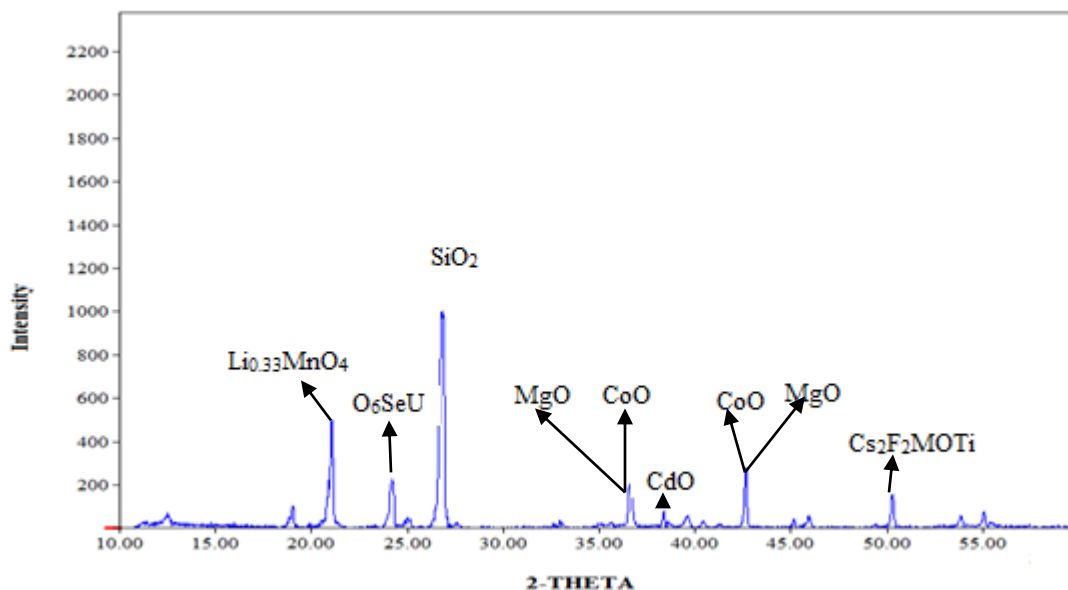


Figure 2 . XRD diagram of Ambo sandstone

4.2 Morphology Characteristics

Scanning electron microscopic (SEM) is widely used for characterization of materials to study the surface morphology, porosity and texture. The surface morphology of Ambo sandstone was shown in Figures 3 . The SEM image with different magnification showed the physical feature of Ambo sandstone. The image indicated that the Ambo sandstone had wide range of grain sizes which ranges from coarse, medium and fine grains. Similar results were reported by Muiayi, (2013) . The investigation of the Figure 3 showed that they have morphology with angular grains of quartz. Similar results were reported for numidian sandstone (Benyamia, 2013). Moreover, as the magnification factor increases, the image size of particular particle increases. But it depends on the voltage used, the spot size and the probe current. To get better resolution , small spot size is needed (Figure 3).

The study by means of SEM does not clearly indicated that the presence of porosity of the Ambo sandstone. This is because the powders used for analysis were not small enough. But as some literature reports show the sandstone has pores eventhough the pores are small (Mounia, 2013). Therefore, it was quartz phase and a mixture of metal oxide phases responsible for adsorption of phosphate ions from aqueous solution with the contribution of porosity. This is according to adsorbents with high iron, aluminum, calcium and manganese contents have high phosphate removing efficiency (Mustefa et al., 2016).

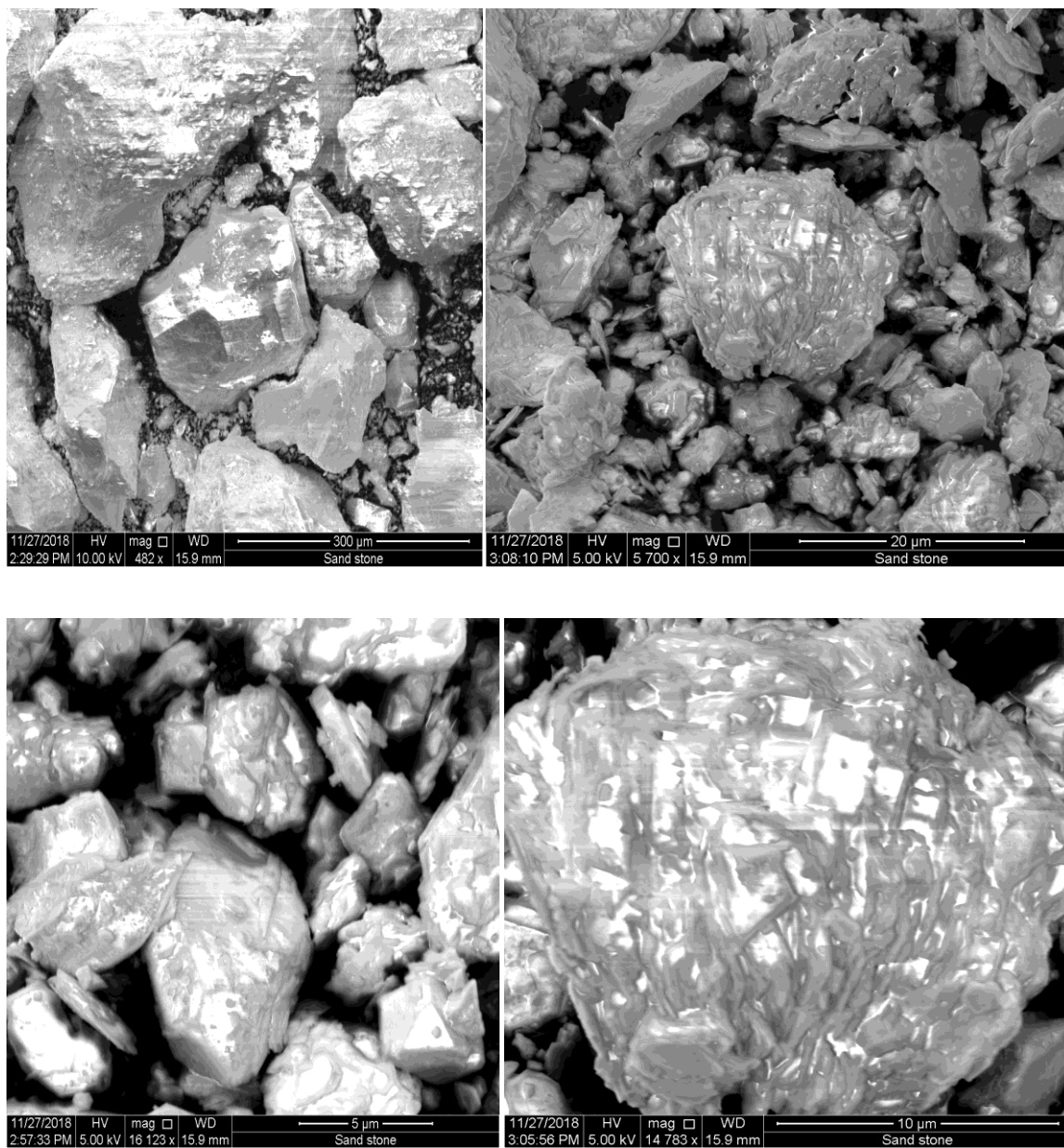


Figure 3 . SEM image of Ambo sandstone.

4.3 Investigation of Adsorption Parameters

4.3.1 Effect of pH

As can be seen from Appendix 2 of Table 2 and Figure 4, the maximum adsorption efficiency (81.99 %) of Ambo sandstone was occurred at pH of 3. The Table also indicated that the highest adsorption capacity (6.15 mg/g) was obtained at the same pH value. Therefore, pH = 3 was the optimum pH for adsorption of phosphate by using Ambo sandstone. The Figure also showed the adsorption efficiency was higher at lower pH (acidic media). This is due to at lower pH more amount of protons present. This intern indicated that the surface of the Ambo sandstone was positively charged. Therefore, columbic attraction forced more PO_4^{3-} from the solution onto the sandstone. The Figure also indicated the curve was declined as the pH increases. This indicated that lower adsorption efficiency was occurred at higher pH values (58.99 % at pH 9). The chemistry behind this is that, as pH increases the concentration of OH^- also increases, which implies the surface of the Ambo sandstone was more negatively charged. So as pH increases the desorption can occur. This may be because columbic repulsion between PO_4^{3-} and OH^- ions. Similar data had been recorded previously for the adsorption of phosphate ions on Fe-Al-Mn on ternary oxide nanosorbent (Buzuayehu, 2012) and on Fe-Al binary oxide nanosorbent (Tofik *et al.*, 2016). The maximum adsorption efficiency was found to be 99.2 % at pH = 4 for adsorption of phosphate from aqueous solution using Fe-Al binary oxide monosorbent (Tofik *et al.*, 2016) whereas pH = 3 was found to be the favorable condition for adsorption of phosphate from aqueous solution using nanosized iron/aluminum/manganese oxide (Buzuayehu, 2012)

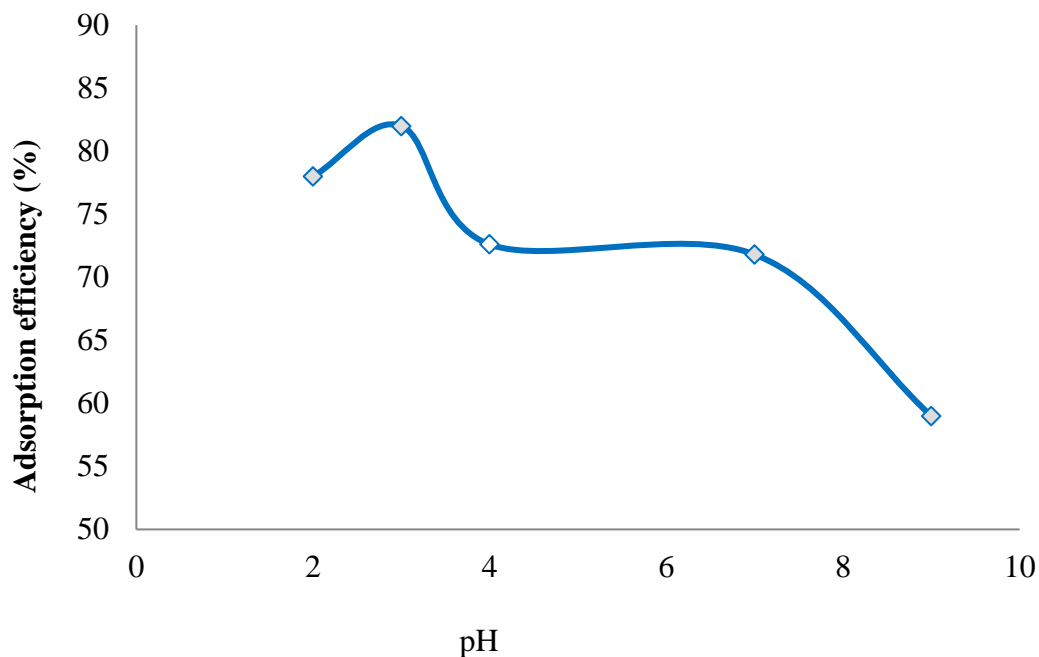


Figure 4. The effect of pH for removal of phosphate (at initial concentration (C_0) = 30 mg/L, dose = 0.1 g, agitation speed = 120 rpm and contact time = 12 h)

4.3.2 Effect of Adsorbent Dose

Most of the scientific studies indicated that phosphorus adsorption increased with increasing adsorbent dose up to a specific level, and then it remained constant. The experimental test results found in Appendix 2 of Table 3 indicated that the maximum adsorption efficiency and the maximum adsorption capacity of Ambo sandstone were 83.37 % and 12.59 mg/g respectively for 0.05 g adsorbent dose used. In supporting this the Figure 5 also showed that, the highest adsorption efficiency (83.37 %) was occurred for lower adsorbent dose used and as the amount of adsorbent used increased, the adsorption efficiency become decreased. This was due to at lower adsorbent dose more surfaces were exposed to the solution (PO_4^{3-}). But as the amount was increased coagulation could occur and adsorption efficiency was decreased. The same results had been found for adsorption of phosphate on water treatment residue (Zelalem, 2014) (Khodadadi *et al.*, 2017).

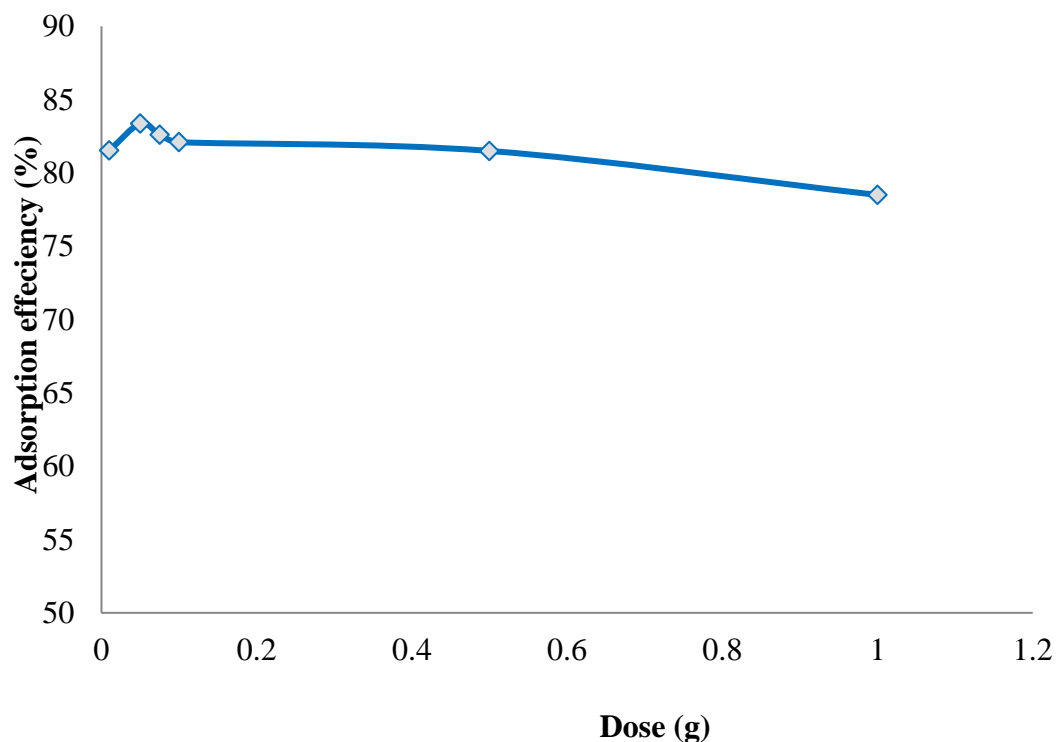


Figure 5. Effect of adsorbent dose on the removal of phosphate (at initial concentration (C_0) = 30 mg/L, pH = 3, contact time = 12 h and agitation speed = 120 rpm)

4.3.3 Particle Size in Phosphate Adsorption

Batch experiment was done by using the particle size of 0.25 mm, 0.300 mm, 0.75 mm and the bulk adsorbents. The particle size in μ have not been sorted because of the lack of sieves in such diameter. As can be seen from the Table 1, the adsorption efficiency of the Ambo sandstone increased from 80 % to 86.46 % when the particle size was decreased from bulk to 0.250 mm. This could happen because as the size of the particle decreases, the surface area increases. This implies that more pore structure would be available. Therefore, adsorption of phosphate ions on and in the surface of adsorbents increases (Do, 2008). Similar results were reported for adsorption of phosphate from aqueous solution by sediments mineral matrices with different particles sizes (0.030, 0.063, 0.092 and 0.125 mm). For these different particle sizes the adsorption capacity was found to increase in the order of 0.125, 0.092, 0.063 and 0.030 mm (Xiao *et al.*, 2013).

Table 1. The effect of particle size for adsorption process

| Particle size | Adsorption efficiency % | Mean residual phosphate concentration (mg/L) |
|---------------|----------------------------|---|
| bulk | 80.00 | 9.51 ± 0.01 |
| 0.750 mm | 84.34 | 7.73 ± 0.01 |
| 0.300 mm | 85.00 | 7.52 ± 0.02 |
| 0.2500 mm | 86.46 | 6.78 ± 0.01 |

4.3.4 Effect of Contact time

Contact time is inevitably a fundamental parameter in all transfer phenomena such as adsorption. The data found in Appendix 2 of Table 4 showed that the maximum adsorption efficiency and the maximum adsorption capacity were 81.29 % and 11.29 mg/g respectively at contact duration of 16 h. As depicted Figure 6, the adsorption efficiency for the first contact time was lower (75.5 %). This is because, in the beginning, only surface adsorption would take place. This instantaneous sorption of adsorbates could be the result of specific chemical interaction or other driving forces like diffusion. But the adsorption % was become increased to 80.5 % when the contact time increased to 12 h. The increase in adsorption rate was because of the relocation of adsorbate ions from boundary layer to the interior porous surfaces. So, transportation rate of the ions from exterior to interior sorption sites determines the rate of adsorption in following phases. Later on, the binding sites became limited and remaining sites were not occupied because of the repulsive forces between adsorbates on solid surface and the bulk phase. Finally, adsorbates removal rate leveled off significantly, which denotes the equilibrium phase (Poudyal, 2015). So as can be seen from Figure 7, the maximum adsorption efficiency 81.29 % was attained at a contact time of 16 h which indicated that process was reached equilibrium. So 16 h was the optimum contact time for adsorption phosphate from aqueous solution using Ambo sandstone. Further when the contact time was increased the adsorption efficiency was almost remain constant. Similar results were found for removal of

phosphate by Zn-Al layered double hydroxides (Küçük, 2017) and the phosphorus uptake by metal-loaded orange waste only reached equilibrium after 15 hr (Biswas *et al.*, 2007).

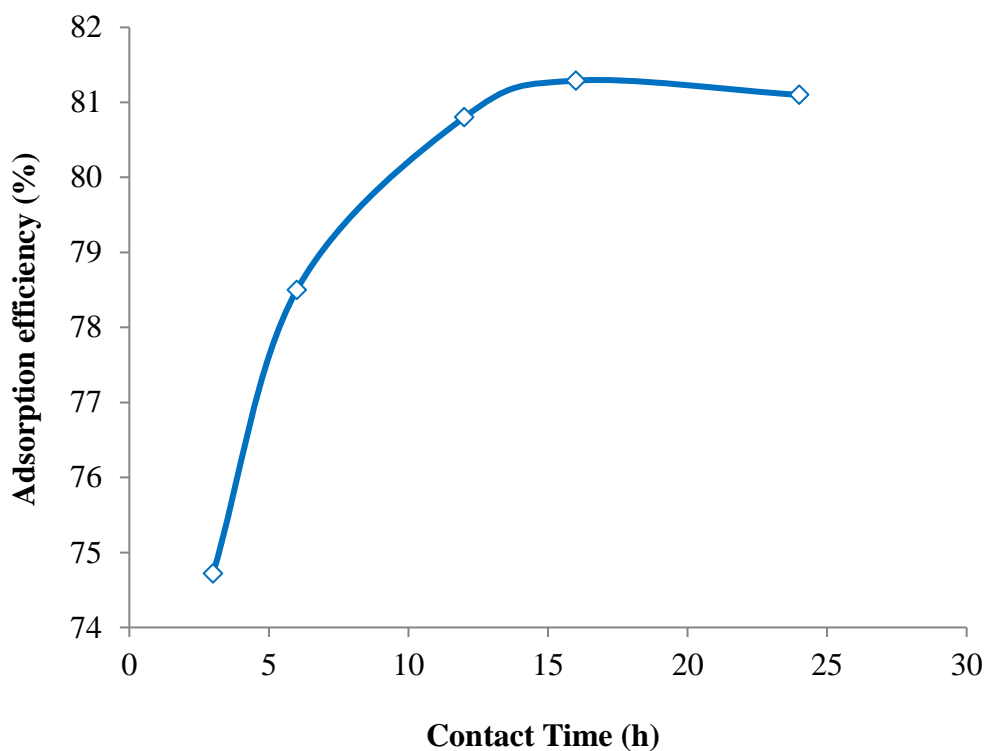


Figure 6. The effect of contact time for removal of phosphate (at initial concentration (C_0) = 30 mg/L, dose = 0.05 g, agitation speed = 120 rpm and pH = 3)

4.3.5 Effect of Speed of Agitation

The optimum agitation speed for adsorption of phosphate ion from aqueous solution was found to be 120 rpm as one can see from the adsorption test results of Appendix 2 of Table 5.

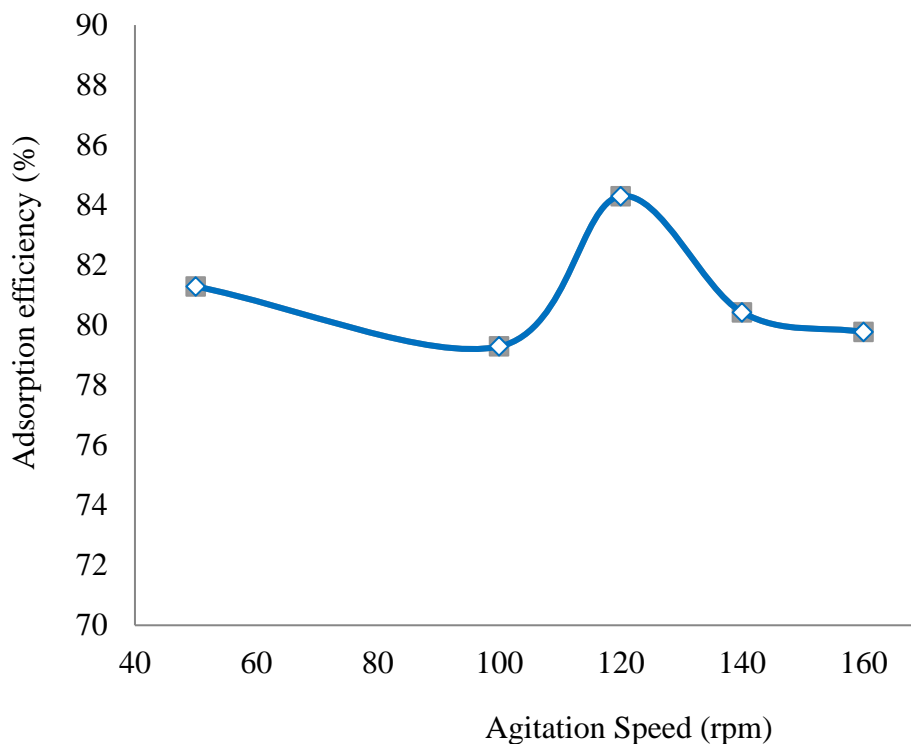


Figure 7. Effect of agitation speed for removal of phosphate (at initial concentration (C_0) = 30 mg/L, pH = 3, dose = 0.05 g and contact time = 12h)

Figure 7 indicated that for the first agitation speed of 50 rpm the adsorption efficiency was high (81.29 %). This is due to film diffusion and more available site of adsorption on the surface of the sandstone. Then when the agitation speed was increased to 100 rpm, the adsorption efficiency became decrease (79.29 %). The possible reason for the observed result was that the surface of the adsorbent had been saturated and desorption might take place. Moreover, the agitation was low and the pore diffusion was not takes place. Later on when the agitation speed was increased to 120 rpm, the adsorption efficiency was also increased to 84.3%. This was due when the stirring speed was high; the thickness of the solvent film layer gets thinner. Therefore, the movement of the phosphate ions through the film layer takes place very fast and the diffusion through the pores becomes the rate controlling step. Finally when the agitation speed was increased further, the adsorption efficiency was started to decrease. This is because with further increase of the agitation speed the already adsorbed phosphate might be desorbed from the adsorption sites (Namasivayam and Sangeetha, 2004).

4.3.6 Effect of Initial Concentration

The effect of initial concentration of adsorbate on the rate of adsorption was investigated by varying the initial concentration of phosphate ions between 10 and 60 mg/L. The results obtained were indicated at Appendix 2 of Table 6. As can be seen from the Table, 76 % was the maximum adsorption efficiency for the initial phosphate concentration of 30 mg/L.

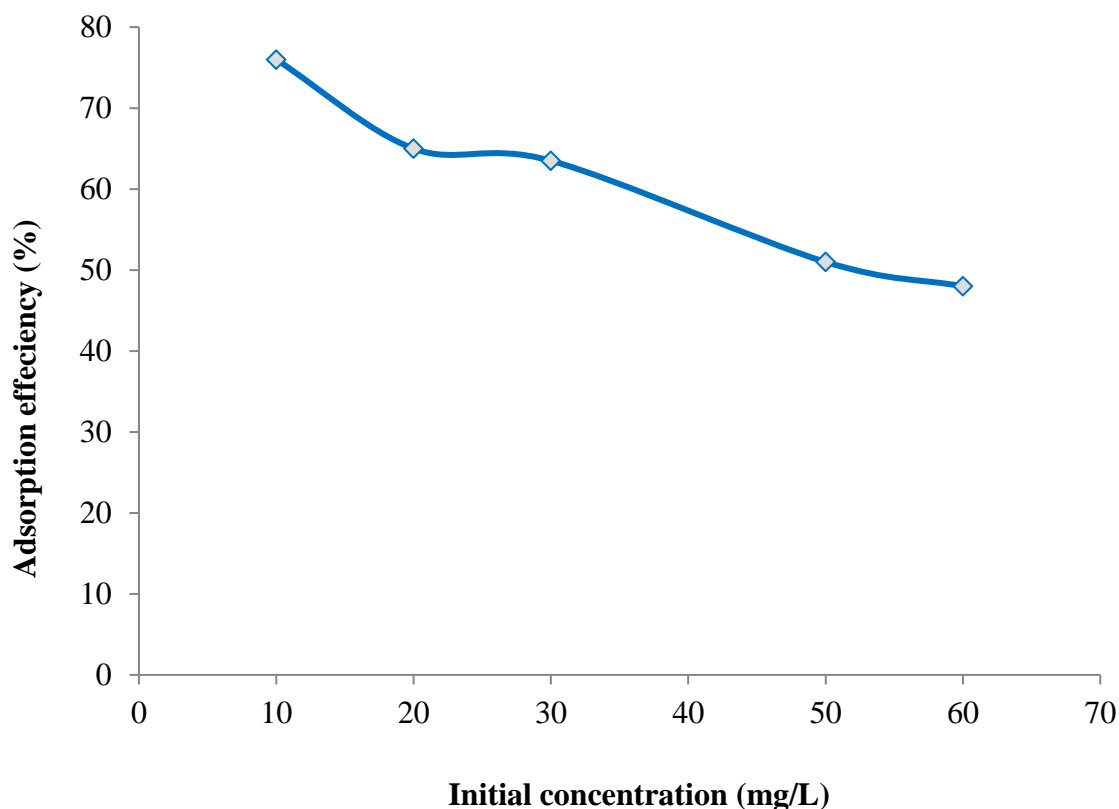


Figure 8. Effect of initial concentration for removal of phosphate (at pH = 3, dose = 0.05 g, contact time = 16 h and agitation speed = 120 rpm)

Figure 8, which illustrated the trend in the sandstone adsorption efficiency with various initial phosphate concentrations of the aqueous solution. As it can be seen from Figure 8, the adsorption efficiency is high (76 %) at the beginning for the initial concentration (10 mg/L) used relative to the others. This was because for the first initial concentration more adsorbing surfaces were available relative to the initial concentration used (Buzuayehu, 2012). As the initial concentration increases from 10 mg/L to 60 mg/L the adsorption

efficiency dropped from 76 % to 44.8 %. This was due to the intra-particle diffusion was takes placed. The reason behind this is the surface of adsorbent and the pores were more saturated and were reached equilibrium. In addition to this the surface of the adsorbent available relative to the concentration is small. The same results had obtained for adsorption of phosphate onto iron hydroxide eggshell (Mezenner and Bensmaili, 2009).

4.4.7 The pH Zero Point Charge

To determine the pH of zero charge, five solutions having pH of 2, 3, 4, 7 and 9 were agitated for 16 h. Then the solutions were withdrawn and the final pH was measured by using pH meter. Finally, ΔpH was calculated by subtracting the initial pH from the final one. Those results are in the Table 2. Based on these results of Table 2, the Figure 10 was plotted using ΔpH vs final pH.

Table 2. Initial, final and change in pH of the pH of zero point charge

| Initial pH | Final pH | ΔpH |
|------------|----------|-------------------|
| 2 | 2.02 | 0.02 |
| 3 | 3.39 | 0.39 |
| 4 | 4.28 | 0.28 |
| 7 | 6.88 | -0.12 |
| 9 | 7.94 | -1.06 |

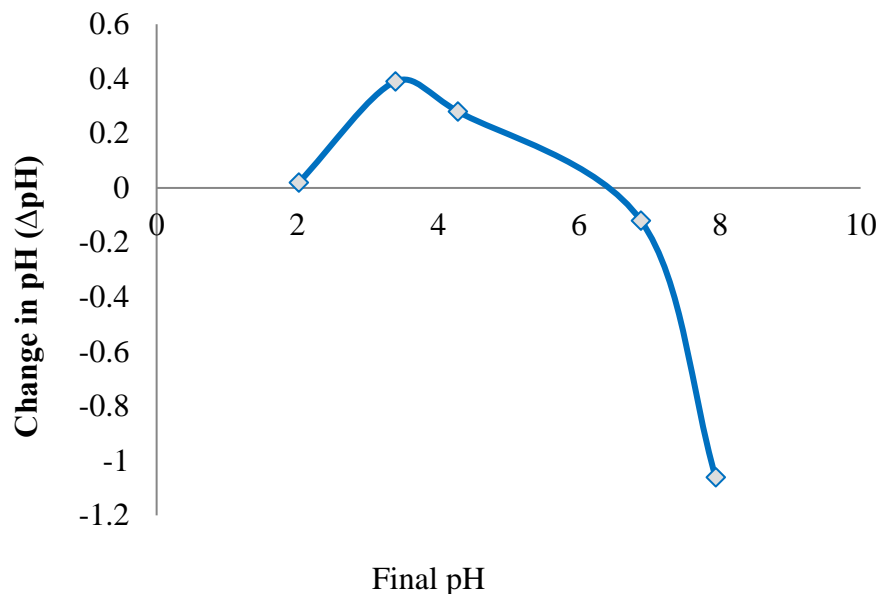
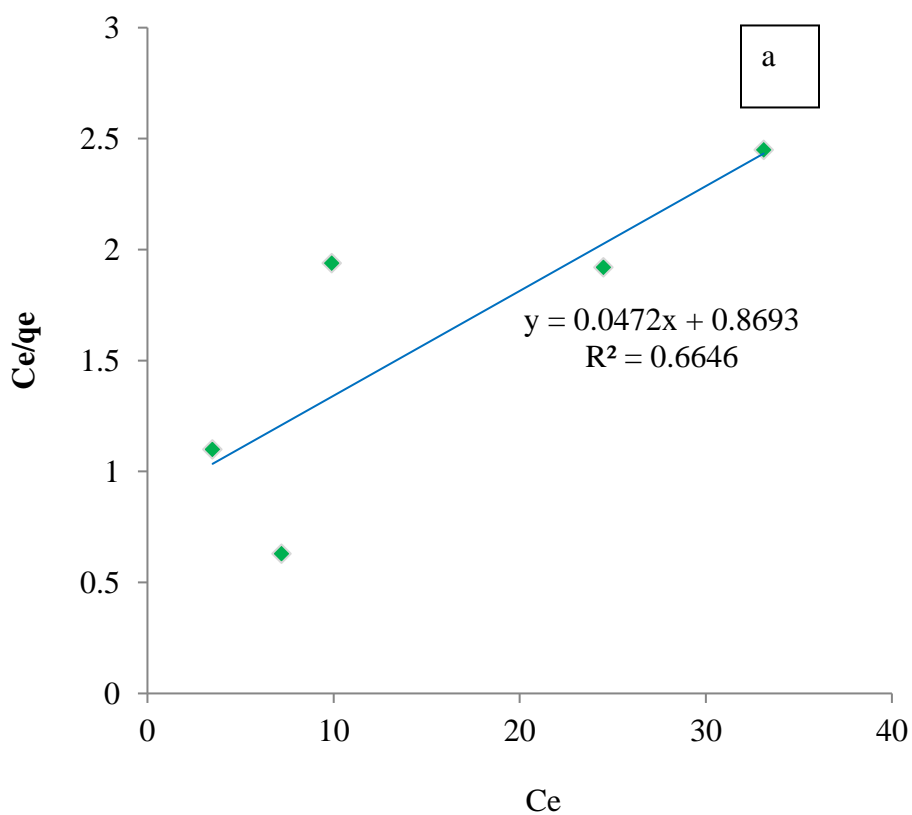


Figure 9. pH_{pzc} of the Ambo sandstone

As can be seen from Figure 9, the curve crosses the horizontal line at about $\text{pH} \cong 6.3$. At this point, the Ambo sandstone surface has a net neutral charge. Theoretically, this unique pH value is known as pH point of zero charge (pH_{pzc}) (Kosmulski, 2002). But this does not mean that the actual point of zero charge. Although there is no net proton surface excess (Preocanin and Kallay, 2005). The sorbent was supposed to exhibit positive charge at $\text{pH} < \text{pH}_{\text{pzc}}$ and negative charge at $\text{pH} > \text{pH}_{\text{pzc}}$ (Figure 10.). Increased protonation was thought to increase the positively charged sites, enlarge the attraction force existing between the sorbent surface and the phosphate anions and thus would more significantly attract the negatively charged monovalent H_2PO_4^- ions in solution and therefore increase the amount of sorption at lower pH (Mengxue *et al.*, 2016). Higher pH value causes the surface to carry more negative charges and thus would significantly electrostatically repulse the negatively charged species in solution, hence the fall in the sorption of phosphate at higher pH (Liu *et al.*, 2008; Mustefa *et al.*, 2016 and Zhang *et al.*, 2005). Therefore, the Ambo sandstone exhibit positive surface charge at $\text{pH} < 6.3$ and a negative surface charge at about $\text{pH} > 6.3$.

4.4 Adsorption Isotherms

The interaction of adsorbent and adsorbate is mainly described in terms of adsorption isotherms to increase the adsorption efficiency of adsorbent. It is based on the assumption that every adsorption site is equivalent and that the ability of a particle to bind there is independent of whether or not adjacent sites are occupied (Langmuir, 1918). In this research, the Langmuir and Freundlich models were employed to describe the experimental data. These experimental results are depicted in the Figure 10 and Table 3.



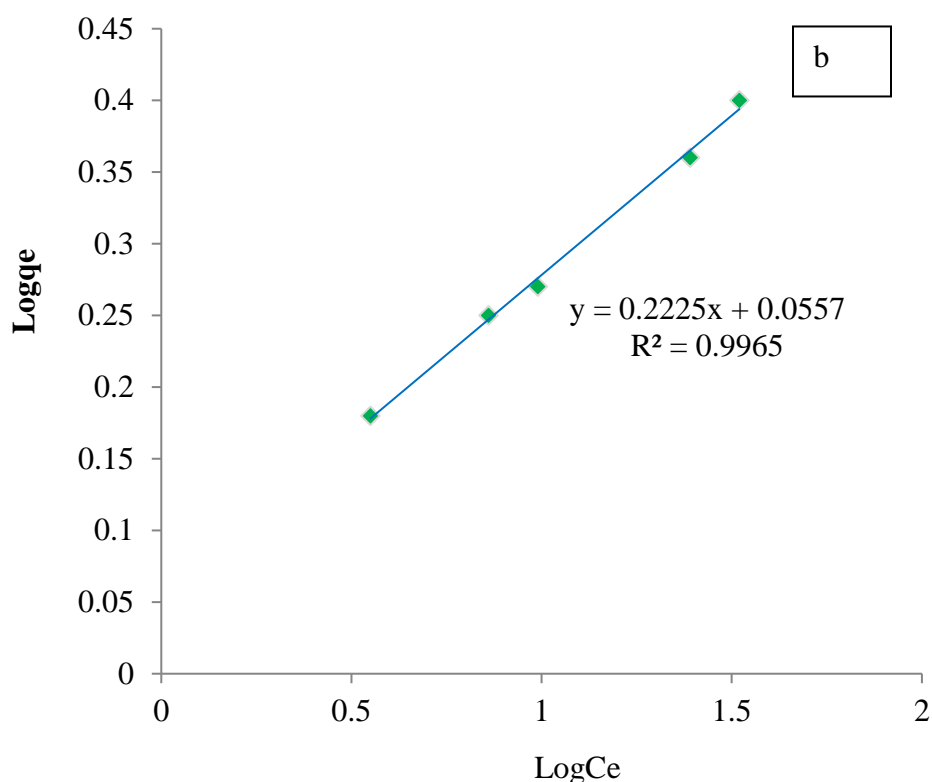


Figure 10. Langmuir (a) and Freundlich (b) adsorption isotherm of phosphate by Ambo sandstone at pH = 3

Table 3. Results for phosphate adsorption isotherms

| Absorbent | Langmuir | | | | Freundlich | | |
|----------------|----------|------|-------|-------|------------|------|-------|
| | q_m | b | R_L | R^2 | n | k | R^2 |
| Ambo sandstone | 21.2 | 0.05 | 0.25 | 0.665 | 4.49 | 1.14 | 0.996 |

4.4.1 Langmuir Isotherm

The Langmuir isotherm was used to test the equilibrium relationship between the amount phosphate ions absorbed onto Ambo sandstone. The equilibrium concentration of phosphate ions and the maximum adsorption capacity of Ambo sandstone were evaluated. Accordingly, the Langmuir constants q_m and b were obtained to be 21.2 (mg/g) and 0.05 respectively (Table 3). They were determined from the linear plot of

C_e/q_e versus C_e (Figure 10 (a)). The high value of b indicates the favorable adsorption process (Hanx *et al.*, 2011). But the value obtained was very small for phosphate ions adsorption with Ambo sandstone. This indicated that the adsorption process was poor. One can see from Figure 10a that the value of $R^2 = 0.665$. This again implied that the adsorption of phosphate by Ambo sandstone was not fitted to the Langmuir model. The essential characteristic of the Langmuir isotherm can be evidenced by the dimensionless constant called equilibrium parameter, R_L .

$$R_L = \frac{1}{1 + bC_0} \quad (12)$$

Where b is the Langmuir constant and C_0 is the initial phosphate concentration, R_L values indicate the type of isotherm to be irreversible ($R_L = 0.$), favorable ($0 < R < 1$), linear ($R_L = 1$) or unfavorable ($RL > 1$). In this study, R_L values fall between zero and one as shown in Table 3. This showed the phosphate adsorption by Ambo sandstone was favorable. The model advocates that uptake occurs on a homogeneous surface by monolayer adsorption without adsorbent molecules interacting (Hameed *et al.*, 2007). It can be concluded from this that the adsorption of phosphate by using Ambo sandstone was not fully homogeneous surface monolayer adsorption.

4.4.2 Freundlich Isotherm

The obtained experimental phosphate ion uptake values have also been analyzed using Freundlich equation. The Freundlich isotherm model is valid for multilayer adsorption on a heterogeneous adsorbent surface with no uniform distribution of heat of adsorption. Freundlich isotherm can be expressed by (Freundlich, 1926).

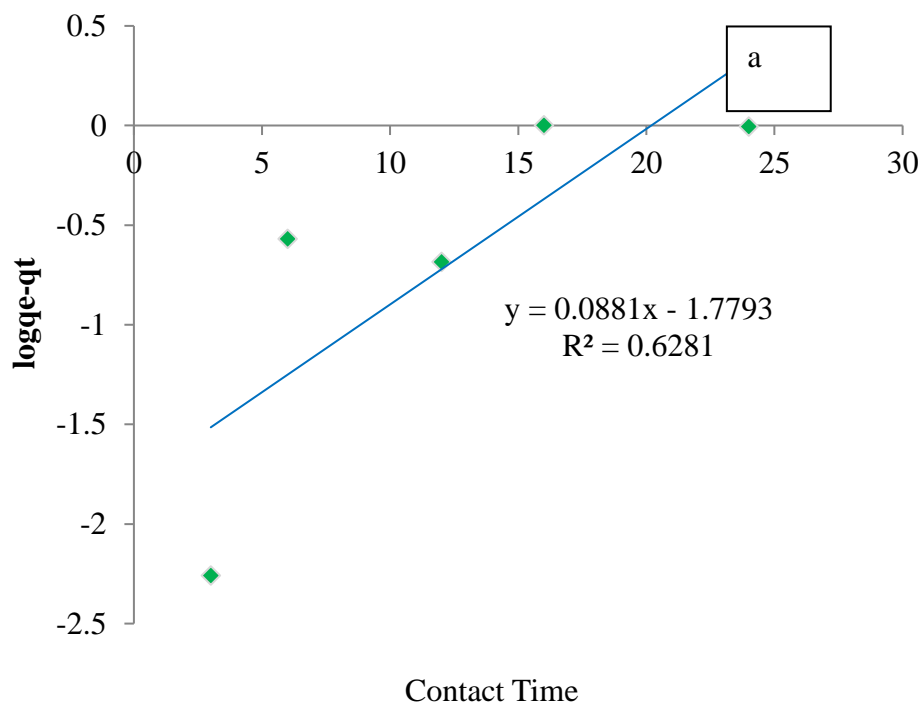
$$\log q_e = \frac{1}{n} \log C_e + \log K_f \quad (13)$$

Where n and K_f are Freundlich constants related to adsorption intensity and adsorption capacity, respectively. The Freundlich constants K_f and n are obtained from the plot of $\log q_e$ versus $\log C_e$ that should give a straight line with a slope of $1/n$ and intercept of $\log K_f$. From Figure 10 b linear relation was observed among the plotted parameters at different concentration. The magnitude of the exponent n gives an indication of the favor

ability of adsorption. It is generally stated that values of n in the range 2–10 represent good, 1–2 moderately difficult, and less than 1 poor adsorption characteristics. For the studied material (Ambo sandstone) the value of n is 4.49 as shown in the Table. Since 4.49 are greater than 2 and less than 10 the adsorption intensity was good. Table 3 showed the calculated values of the Langmuir and Freundlich models' parameters. The comparison of correlation coefficients values (R^2) of the linearized form showed that the Freundlich model yields ($R^2 = 0.997$) a better fit for the experimental adsorption equilibrium data and the most appropriate isotherm to describe the equilibrium date of phosphate adsorption by Ambo sandstone. This also confirmed that the surface of Ambo sandstone is heterogeneous, with different energy of distribution sites.

4.5 Kinetics Studies

Since adsorption is dependent on time it is very important to know the rate of adsorption. So the removing ability of the adsorbent can be evaluated. Accordingly, the adsorption of capacity of Ambo sandstone was evaluated based on Lagergren's and Ho's theory.



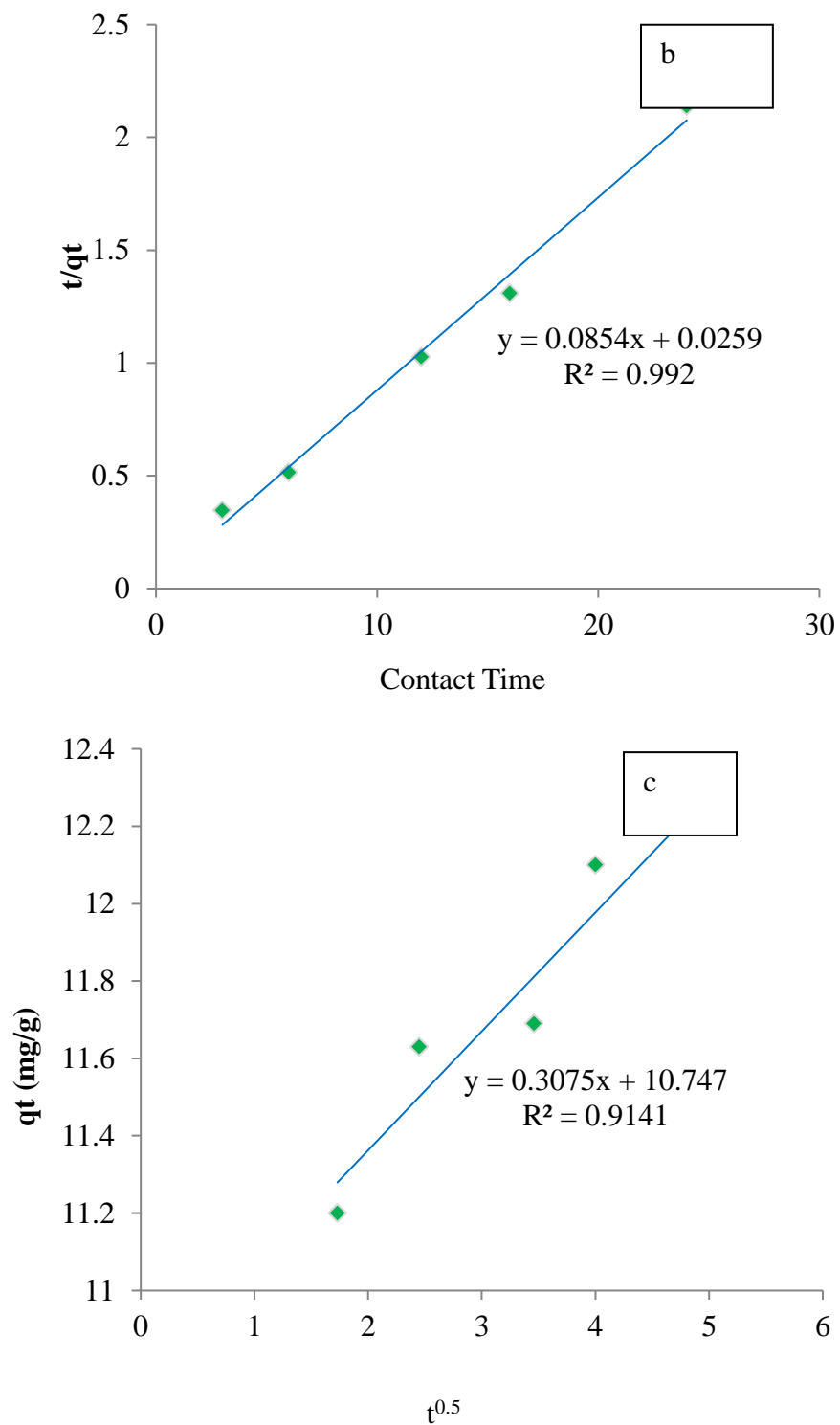


Figure 11. Pseudo-first order (a), pseudo-second order (b) and intra-particle diffusion model (c) adsorption kinetics of phosphate by Ambo sandstone at pH = 3

From pseudo-first-order plot the rate constants k_1 and the adsorption capacity were determined and found to be 0.088 and 5.91 mg/g; respectively. From the Figure 11 (a) and Table 4 it can be seen that, the correlation coefficient is 0.628 which is very small. This indicated that the pseudo-first order was not well fit the adsorption of phosphate by using Ambo sandstone. The experimental results were also treated to determine the relation between rate of adsorption and time for pseudo-second order kinetics. This was well indicated by linear plot of t/q vs t . From the graph 11 (b) and Table 4 the correlation coefficient (R^2) was found to be 0.996, indicating that the adsorption of phosphate using Ambo sandstone well obeyed pseudo second order model kinetic sorption process. It was also indicated that more of the adsorption process might be chemisorptions.

In chemisorptions the adsorbate (phosphate) attached to the adsorbent (Ambo sandstone) by forming usually covalent bond. In addition to this q_e of the calculated one (11.7) was closed to the experimental value (12.2). This means the adsorption rate was related to the concentration of the activated sites on the surface of the Ambo sandstone. So this showed that the adsorption of phosphate from aqueous solution using Ambo sandstone better correlated with pseudo-second order kinetics than pseudo first-order kinetics. The pseudo first-order does not fit well with the whole range of contact time and usually applicable only over the initial stage of process (Hammeed *et al.*, 2007). Whereas pseudo second-order kinetic model based on adsorption equilibrium capacity and the model can be used to predict the behavior over the range of adsorption (Ho and McKay, 1999 and Liu, 2008).

Adsorption is a multi-step process involving the transport of the solute molecules from the aqueous phase to the surface of the solid particulate followed by diffusion of the solute molecules into the pore interiors (Weber and Morris, 1963). According to this theory the adsorption of phosphate from aqueous solution using Ambo sandstone was tested against interparticle diffusion model and the plot of Figure 11 (c) was obtained. As can be seen from the Figure, the straight line was not passed through the origin and some points were deviated from the straight line. The deviation of the straight line from the origin might be due to the difference in the rate of mass transfer in the initial and final stages of adsorption (Panday *et al.*, 1986). The value of the slope ($K_{ist} = 0.308$) which w

as small indicated that the pores are microspores and the interior particle diffusion resistance was due to microspore. In addition to this the value of the intercept (10.74) which were greater zero, also indicated that the mode of transport was affected by more than one process (Hameed, 2009). The correlation coefficient ($R^2 = 0.9141$) was somewhat high showing that the adsorption of phosphate using Ambo sandstone was follow intra-particle diffusion model. Therefore, it might be concluded that surface adsorption and intra-particle diffusion were concurrently operating during adsorption of phosphates (Dhaba, 2013).

Table 4. The values of parameters and correlation coefficients of kinetic model

| Model | K | R^2 | q_e (mg/g) |
|--------------------------------|--------|--------|--------------|
| Pseudo-First-Order | 0.0881 | 0.6281 | 5.91 |
| Pseudo-Second-Order | 0.259 | 0.9962 | 11.70 |
| Inter-particle diffusion model | 0.3075 | 0.9141 | 11.8 |

4.6 Thermodynamics of Adsorption

Adsorption is affected by the relations between the properties of the adsorbent and the solute. Thus, the effects of temperature are different for different adsorbents and solutes. In addition the temperature affects the thermodynamics parameters like free energy, entropy and enthalpy. These parameters are valuable to look into the feasibility and spontaneous nature of the adsorption process. Based on this idea, experiments were done on adsorption of phosphate from aqueous solution by using Ambo sandstone. The results indicated that, the adsorption efficiency increased from 59.3% to 68.5% as temperature was increased from 30 to 60 °C. Similar results had been found by different researchers. Among them, Saha *et al.* (2010) found that at pH 3, the maximum amount of phosphate adsorbed per gram of added granular ferric hydroxide occurred at 45 °C. Mezenner and Bensmaili (2009) showed that the phosphorus adsorption capacity of iron hydroxide eggshell increased as the solution was heated from 20 to 45 °C. Benyoucef and Amrani

(2011) attributed the higher phosphorus adsorption capability with increasing temperature to the expansion of pore size at higher temperatures.

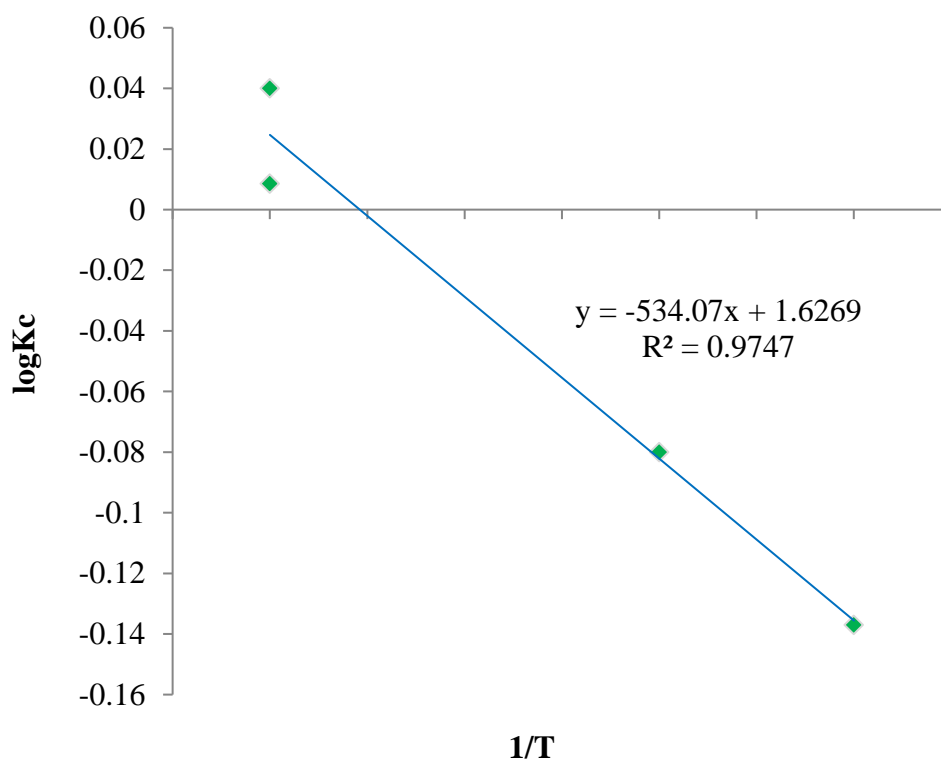


Figure 12. Plot of $\ln K_c$ Vs T^{-1} for phosphate adsorption (pH = 3, dose = 0.05 g, agitation speed = 120 rpm, Contact time = 16 h, $C_o = 50$ mg/ L)

From the linear plot of $\text{Log}K_c$ vs T^{-1} and using the slope and the intercept of the graph, the value of ΔH was calculated to be 0.4 KJ/mol k and that of ΔS was found to be 13.5 J/mol.k. Using the values of ΔH and ΔS , the value of ΔG was tabulated in the Table 5 at different temperature. The Table showed that all the values of ΔG were negative indicating that the feasibility and spontaneously of the adsorption of phosphate by the Ambo sandstone. Moreover, the positive values of enthalpy change indicated that the adsorption process was endothermic. Which means the adsorption process mainly involved the chemical phenomenon.

Table 5. Thermodynamic parameters for phosphate adsorption onto Ambo sandstone adsorbent

| T(K) | ΔG (KJ/mol) | ΔH (KJ/mol k) | ΔS (J/mol k) |
|------|---------------------|-----------------------|----------------------|
| 303 | -3.6 | 0.444 | 13.5 |
| 313 | -3.78 | | |
| 323 | -3.9 | | |
| 333 | -4.1 | | |

4.7 Interfering Ions

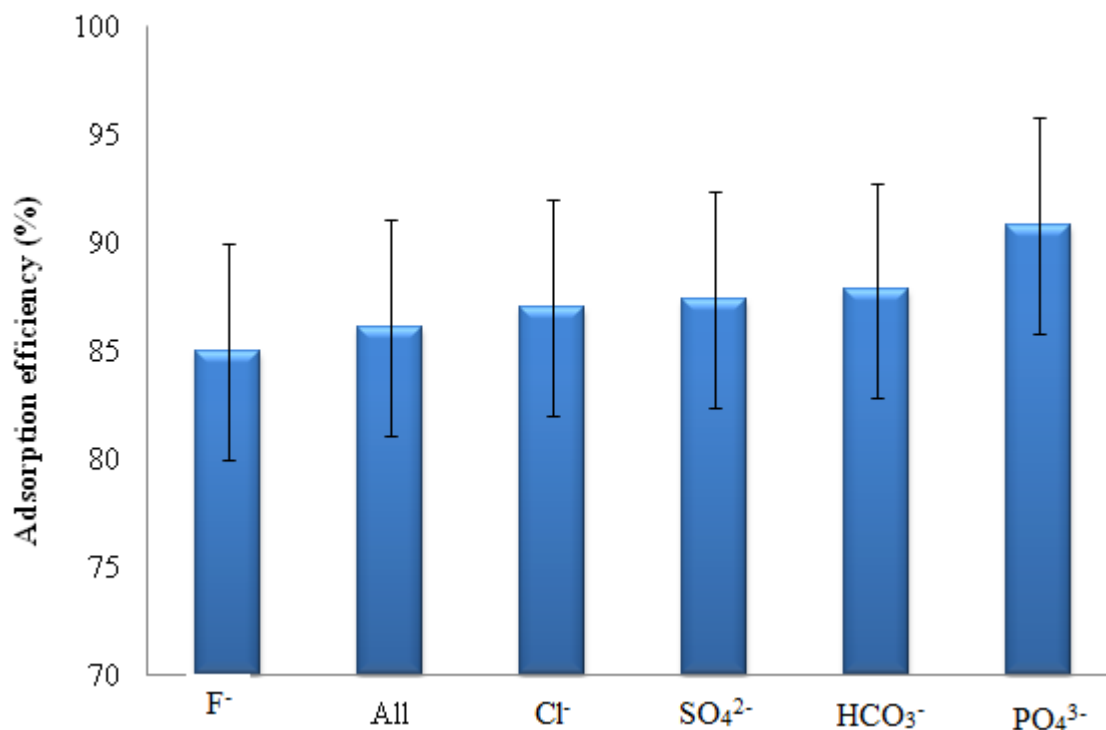


Figure 13. Effect of anions on phosphate Adsorption

Adsorption experiments were conducted by preparing phosphate solution of 30 ppm and 30 ppm of each PO₄³⁻, HCO₃⁻, SO₄²⁻, Cl⁻, F⁻ and the mixture of all. The experiments were done by mixing 7.5 mL of PO₄³⁻ and 7.5 mL of each ions in separate flask making a total volume of 25 mL having pH = 3, agitation speed = 120 rpm, contact time = 16 h and adsorbent dose = 0.05 g. Based on this experiment different results were obtained. As

indicated in the Figure 13, all anions interfere with the adsorption efficiency. Among the ions indicated, the presence of F^- decreased the adsorption efficiency from 90.82% to 85%, which was very high. This indicates that the interaction between fluoride and Ambo sandstone is feasible. Similar results has been found for the interaction between fluoride and nano-alumina moieties is feasible (Seiram and Meenakshi, 2009). Regarding this many researchers have studied potential effects of various ions on the adsorption efficiency of phosphate ion from wastewater. Divya *et al.* (2012) stated that the presence of anions like Cl^- , SO_4^{2-} , NO_3^- and CO_3^{2-} did not show any significant influence on phosphate adsorption, whilst some cations such as Ca^{2+} , Mg^{2+} , Cu^{2+} , Fe^{2+} and Zn^{2+} facilitate the process. These findings coincide with those reported by Chen *et al.*, (2014). They concluded that anions of Cl^- , NO_3^- and SO_4^{2-} had a negligible effect on phosphorus adsorption by natural pyrite. On the other hand, a study conducted by Zhang *et al.* (2012) showed that SO_4^{2-} and CO_3^{2-} had a negative influence on the phosphate uptake of lanthanum-doped activated carbon fiber. These results demonstrated the complex nature of adsorption process, especially when competing ions are involved. Therefore, the effect of different anions on phosphate adsorption from wastewater depends not only on the nature of anions but also on the nature of adsorbents involved. The results correlate with this complex nature of the adsorption process (Bashan and Bashan, 2004).

4.8 Desorption of Phosphate

The most suitable adsorbent is not the one which has only the highest capacity to adsorb adsorbate but should also has capacity to release the adsorbed adsorbate. The most common desorbing agents for desorption of phosphates are salts, acids and bases (Loganathan *et al.*, 2006). In this study acids and bases were employed for desorption of phosphate from Ambo sandstone. Based on the experimental results (Figure 17), the desorption of phosphate was lower (20 %) at lower pH. This is due to at lower pH phosphate predominantly present in an un-ionized form ($H_2PO_4^-$). Especially the lowest desorption efficiency (18.9 %) was occurred at pH 3. This might be high concentration of $H_2PO_4^-$. As can be observed from the Figure 14 again as pH increase from 3 to 9 desorption efficiency increases from 18.9 % to 22 %. This was due to the increase number of OH^- ions present at high pH which competes with phosphate ions

(Namasivayam1 and Wolfgang, 2005). But even though the desorption was increased as pH increased, in general the % of desorption was small. This was might be due to strong bond between the adsorbent and the phosphate ion; chemisorptions might be involved in the process (Buzuayehu, 2012).

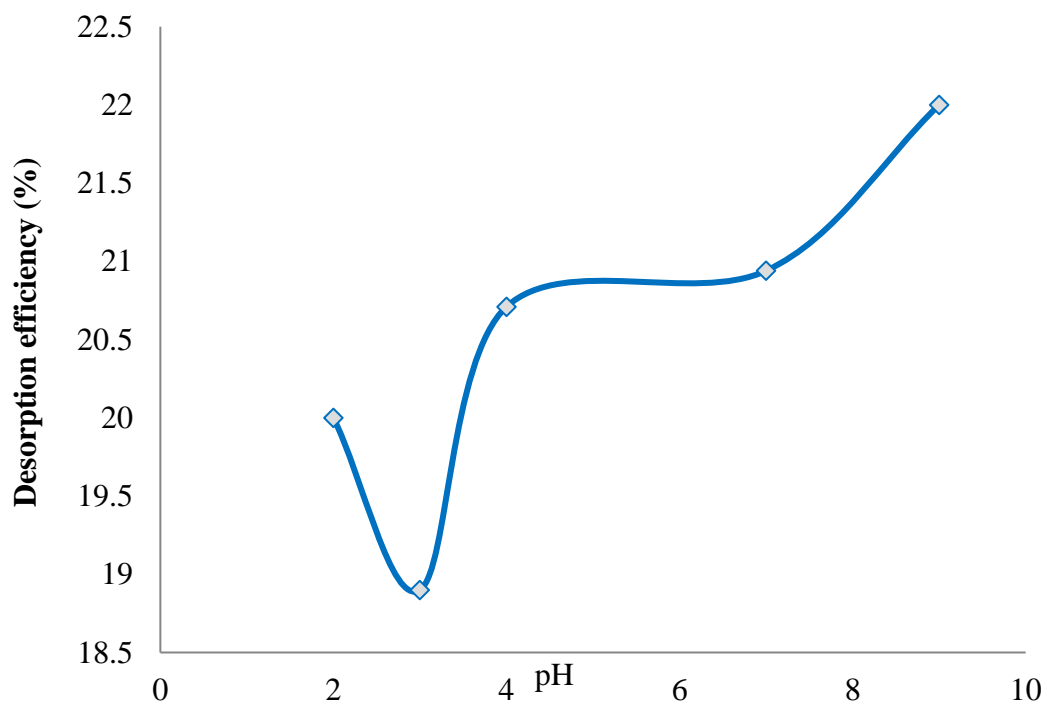


Figure 14. Desorption of phosphate ions from Ambo sandstone using acids and bases.

5. CONCLUSIONS AND RECOMMENDATIONS

5.1 Conclusion

Phosphorus as phosphates is used by plants and animals. Many factories and detergent industries use phosphates. But due to poor management practice they release excess phosphates in to water bodies which causes accelerated growth of algae (eutrophication). Because of this many attempts have been made to remove phosphates from wastewater using different materials. This study was tried to remove phosphate from aqueous solution by using easily manageable, cost effective and readily available Ambo sandstone. Ambo sandstone was used to adsorb phosphates from aqueous solution without any chemical modification. Based on the experimental results, the following points can be concluded.

- The characterization results of SEM and XRD revealed the roughness and the crystalline structure of the Ambo sandstone respectively. Furthermore the XRD analysis indicated that the stone mainly composed of quartz (SiO_2) and a mixture of oxides which was mainly responsible for the adsorption of the phosphate ions from aqueous solution concurrently with the porosity.
- The Ambo sandstone was optimized with respect to different parameters. The optimum values obtained for the parameters evaluated were: contact time = 16 h, pH = 3, adsorbent dose = 0.05 g, particle size = 0.25 mm and initial phosphate concentration = 30 mg/L.
- Again the adsorption process was evaluated against Langmuir and Freundlich models and the adsorption of phosphate from aqueous solution using Ambo sandstone well fitted the Freundlich model.
- The kinetics models such as pseudo first-order, pseudo second-order and intra-particle diffusion models were investigated and the process was found to obey the pseudo-second –order model.

- To see the spontaneity of the adsorption of phosphate from aqueous solution using Ambo sandstone, the process was carried out at different temperature and the process was found to be spontaneous.
- Lastly, the point of zero charge and the desorption process were evaluated and the point of zero charge obtained was 6.3 and the desorption efficiency was small.

5.2 Recommendation

In this study, the Ambo sandstone removal efficiency of phosphate ions from aqueous solution was determined. But for practical application, some conditions to be considered further are:

- ✚ Since the adsorption efficiency determined was moderate, other research should be conducted by activating the sandstone to enhance adsorption efficiency.
- ✚ Real wastewater treatment that contain phosphate ion should undertaken by using the stone to see the selectivity of the adsorbent with heavy metals should carried out.
- ✚ Removal efficiency of the sandstone through continuous column experiment can be checked.
- ✚ The removal efficiency of the sandstone for other anions has to be performed.

6. REFERENCES

- Abdul K. , Sri Aprilia , N.A , Bhat . A.H, Jawaid . M, Paridah . M.T and Rudi. D. A, 2013. Jatropha biomass as renewable materials for biocomposites and its applications. *Renewable and Sustainable Energy Reviews*, 22: 667–685.
- Akpor,O.B. and Muchie M., 2010. Bioremediation of polluted wastewater influent : Phosphorus and nitrogen removal. *Scientific Research and Essays*, 5: 3222-3230.
- Amuda , O.S. and Ibrahim A.B., 2006. Industrial wastewater treatment using natural and modified materials. *Annual Review of Energy and Environment*, 25: 53-88.
- Andrea B., and Marco A. , 2014. Bamboo based activated carbon: Kinetics and equilibrium studies. Aqueous solutions, 63 75, *Journal of Hazardous Materials*, 141: 819 - 825.
- Arcadio, P. and Gregoria A., 2003. Physical Chemical Treatment of Water and Wastewater.
- Benyamina Mounia, Boucheur Merzoug, Benabbas Chaouki, and Ait Abdelouahab Djaouza et al., 2013. *IACSIT International Journal of Engineering and Technology*, 5(1).
- Benyoucef, S. and Amrani, M., 2011. Adsorption of phosphate ions onto low cost Aleppo pine adsorbent. *Desalination*, 275: 231–236.
- Biazen, B., 1962. Generalized report about the geological view of Ambo and Guder. Ministry of Mines and State Domain, Addis Ababa, unpublished report.
- Biswas, B.K., Inoue, K., Ghimire, K.N., Harada, H., Ohto, K. and Kawakita, H., 2008. Removal and recovery of phosphorus from water by means of adsorption onto orange waste gel loaded with zirconium. *Bioresource Technology*, 99(18): 8685-8690.

- Blaney, L.M., Cinar, S., and Sengupta, A.K., 2007. Hybrid anion exchanger for trace mcandidate umami receptor taste-mGluR4, in taste cells. *Chemical Senses*, 28: 559 – 565.
- Buzuayehu Abebe, Abi M. Tadesse, Tesfahun Kebede, Endale Teju and Isabel Diaz., 2017. Fe Al-M ternary oxide nanosorbent: Synthesis, characterization and phosphate sorption property, *Journal of Environmental Chemical Engineering*, 5: 1330–1340.
- Caravelli, A.H., Contreras E.M., and Zaritzky N.E., 2010. Phosphorus removal in batch systems using ferric chloride in the presence of activated sludges. *Journal of Hazard Materials*, 172: 199–208.
- Carpenter, S. R., 1998. Nonpoint pollution of surface waters with phosphorous and nitrogen. *Ecological Applications*, 8: 559 - 568.
- Cecen, F. and Aktas, O., 2012. Activated Carbon for Water and Wastewater Treatment. Integration of Adsorption and Biological Treatment. Germany : Wiley-VCH.
- Chaudhari, N., Pereira, E., Landin, A.M. and Roper, S.D., 2003. Immuno detecting a column in series. *Separation Science and Technology*, 47: 1785 - 1792.
- Crittenden, B. and Thomas, J., 1998. Adsorption technology and design. Oxford: Butterworth-Heinemann.
- De- Bashan, L.E. and Bashan, Y., 2004. Recent advances in removing phosphorous from wastewater and its future use as fertilizer . *Water Research*, 38: 4222-4246.
- Dhaba Abera, 2013. Kinetics studies on adsorption of lead and cadmium on powder and activated carbon of weed plant parthenium hysterophorus, Haramaya University.
- Divya, J.M., Rohini, K. K. and Ravindhranath, K., 2012. Phosphate pollution control in waste water using new bio-sorbents. *International Journal of Water Resources and Environmental Engineering*, 4: 73-85.
- Do, D., 2008. Adsorption analysis. 1st ed. London: Imperial College Press.
- Duenas, J.F., Alonso, J.R., Rey, A.F. and Ferrer, A.S., 2003. Characterisation of phosphorous forms in wastewater treatment plants. *Journal of Hazard Materials*, 97: 1–3.

- Ehssan., 2012. Removal of Phosphates from Industrial Waste Water by Chemical Precipitation. *IRACST – Engineering Science and Technology. An International Journal (ESTIJ), ISSN, 2: 2250-3498.*
- Everglade hub, 2013. Phosphorous removal technologies. Available <http://www.evergladeshub.com/okeechobee>.
- Fei L., Ji-Lai G., Guang-Ming Z., Long C., Xi-Yang W., Jiu-Hua D., Qiu-Ya N., Hui-Ying Z. and Xiu-Rong Z., 2011. Removal of phosphate from aqueous solution by magnetic Fe–Zr binary oxide, *Chemical Engineering Journal, 171: 448-455.*
- Freundlich, H., 1926. *Colloid and capillary Chemistry.* Methuen, London.
- Gérard.F., 2016 . Clay minerals, iron/aluminum oxides, and their contribution to phosphate sorption in soils a myth revisited. *Geoderma, 262: 213–226.*
- Gupta, M.D., Loganathan, P., and Vigneswaran, S., 2012. Adsorptive removal of nitrate and phosphate from water by a Purolite ion exchange resin and hydrous ferric oxide columns in series. *Separation Science and Technology, 47: 1785 – 17.*
- Hameed, B.H., Din A.T.M., and Ahmad . A.L., 2006. Adsorption of methylene blue onto bamboo-based activated carbon: Kinetics and equilibrium studies. *Journal of Hazardous Materials, 141: 819–825.*
- HAN, X., WANG, W. and MA, X., 2011. Adsorption characteristics of methylene blue onto low cost biomass material lotus leaf. *Chemical Engineering Journal, 1: 171.*
- Harvey, O.R. and Rhue. R.D., 2008. Kinetics and energetic of phosphate sorption in a multi-component Al(III)-Fe(III) hydr (oxide) sorbent system. *Journal of Colloids Interface Science , 322: 384–393.*
- Hesselmann, R., Hummell, R., Resnick, S., Hany, R. and Zehnder, A., 2000. Anaerobic metabolism of bacteria performing enhanced biological phosphate removal. *Water Research, 34: 3487-3494.*
- Ho, Y.S. and McKay, G., 1998. Kinetic models for the sorption of from aqueous solution by wood. *Journal of Environmental Science Health Part B: Process Safety Environ. Protect, 76: 183–191.* <http://www.water.rutgers.edu/Projects/trading/p-trt-lit-rev-2a.pdf>. (Accessed on January 4, 2013).

- Indra, D., Vimal C., Nitin, S. and Agarwa, K., 2006. Removal of Orange-G and Methyl Violet dyes by adsorption onto bagasse fly ash—kinetic study and equilibrium isotherm analyse. *Dyes and Pigments*, 69: 210-223.
- Jones, C. 2013. Core evaluation and clay analysis of the Newcastle Sandstone, Osage Wyoming. Prepared for Osage Partners, LLC By EOR.
- Karageorgiou ,K., Paschalis. M., and Anastassakis.G.N., 2007. Removal of phosphate species from solutions by adsorption onto calcite used as natural adsorbent. *Journal of Hazard Materials*, 139: 447–452.
- Kawakita, H., 2007. The adsorption of phosphate from an aquatic environment using metal-loaded orange waste. *Journal of Colloid and Interface Science*, 312: 214-22.
- Kosmulski, M., 2002. The pH-Dependent Surface Charging and the Point of Zer Charge. *Journal of Colloid Interface Science*, 253: 77-87.
- Kucuk Mehmet 2017. Removal of sulfate and phosphate by Zn-Al layered double hydroxides. Master's Thesis, Lappeenranta University of Technology.
- Kumar, P., Sudha, S., Chand, S. and Srivastava, V. C., 2010. Phosphate Removal from Aqueous Solution Using Coir-Pith Activated Carbon. *Separation Science and Technology*, 45: 1463–1470.
- Lalley, J., Han, C. Li, X., Dionysiou, D.D. and Nadagouda. M.N.,2016. Phosphate adsorption using modified iron oxide-based sorbents in lake water: kinetics, equilibrium, and column tests, *Chemical Engineering Journal*, 284: 1386–1396.
- Lefebvre, D. and Tezel, F., 2017. A review of energy storage technologies with a focus n adsorption thermal energy storage processes for heating applications. *Renewable and Sustainable Energy Reviews*, 67: 116-125.
- Liu, H., X. Sun, C. Yin, and C. Hu, 2008. Removal of phosphate by mesoporous ZrO₂, *journal of hazard.materials*, 151: 616–622.
- Loganathan, P., Vigneswaran, S., Kandasamy, J., and Bolan, N.S., 2014. Removal and
- Maryam, K., Aliyeh, H., Lida, R., Hadighe, D.,and Negin Nasseh, 2017. Removal of Phosphate from Aqueous Solutions by Iron Nano-Magnetic Particle Coated with Powder Activated carbon. *Journal of Health Science and Technology*, 1: 17-22.
- McKay, C.P., 1996. Elemental composition, solubility, and optical properties of Titan's

- Meftah, T. and Zerafat, M. M., 2016. Nitrate Removal from Drinking Water using Organo Silane Modified Natural Nano Zeolite. *International Journal of Nanoscience Nanotechnol*, 12: 223-232.
- Mengxue, Li., Jianyong, L., Yunfeng X., and Guangren, Q., 2016. Phosphate adsorption on metal oxides and metal hydroxides: A comparative review, School of Environmental and Chemical Engineering, Shanghai University.
- Mezenner, Y. N. and Bensmaili, A., 2009. Kinetics and thermodynamic study of phosphate adsorption on iron hydroxide-eggshell waste. *Chemical Engineering Journal*, 147: 87–96.
- Mubiayi Mukuna P., 2013. Proceedings of the World Congress on Engineering , III London, U.K.
- Mullins, G., 2009. Phosphorous, Agriculture and Environment. *Available at Mineralogical Magazine*, 72: 337–340.
- Namasivayam, C. and Sangeetha, D., 2004. Equilibrium and kinetic studies of adsorption of phosphate onto ZnCl₂ activated coir pith carbon, *Journal of Colloid Interface Science*, 280: 359–365.
- Oelkers, E.H., Valsami-Jones, E., and Roncal-Herrero, T., 2008. Adsorption of phosphate onto activated carbon. *Chemical Engineering Science*, 36 : 721 - 730.
- Panday, K., Prasad, G. and Singh, V., 1986. *Mixed adsorbents for Cu (II) removal from aqueous solutions*. *Environmental Technology*, 7: 547-554.
- Peleka, E.N. and Deliyanni, E.A., 2009. Adsorptive removal of phosphates from water and wastewater. *Water Research*, 41: 1603 - 1613.
- Poudyal Manisha, 2015. Investigation on the Efficiencies of Low Cost Adsorbents for the Treatment of Fluoride Contaminated Water.
- Preocanin, T. and Kallay, N., 2006. Point of Zero Charge and Surface Charge Density of TiO₂ in Aqueous Electrolyte Solution as Obtained by Potentiometric Mass Titration, *Croatia Chemistry Acta*, 79: 100-104.
- Ragothama, K. G., 1999 . Annual Review of Plant Physiology and Plant recovery of phosphate from water using sorption. *Critical Reviews in Environmental Science and Technology*, 44: 847 - 907.

- Rehab, M., Hesham, A., Mohamed M., and Gihan F., 2016. Potential of using green adsorbent of heavy metal removal from aqueous solutions, Adsorption kinetics, isotherm, thermodynamic, mechanism and economic analysis, *Ecological Engineering*, 9: 317-332.
- Rodrigues, L. and da Silva, M., 2009. An investigation of phosphate adsorption from aqueous solution onto hydrous niobium oxide prepared by co-precipitation method. *Colloids and Surfaces A. Physicochemical and Engineering Aspects*, 334: 191-196.
- Rybicki, S.M., 1998. New technologies of phosphorous removal from wastewater. Available at <http://www2.lwr.kth.se/forskningsprojekt/Polishproject/JPS3s121.pdf>. (Accessed on January 3, 2013).
- Saha, B., Griffin, L. and Blunden, H., 2010. Adsorptive separation of phosphate oxyanion from aqueous solution using an inorganic adsorbent. *Environmental Geochemistry and Health*, 32: 341-347.
- Schindler, D.W., 1974. Eutrophication and recovery, in environmental lakes : *Implication for lake management Science*, 184: 894-899.
- Schindler, D.W., Armstrong, F.A., and S.K., G.J., 1971. Eutrophication of lake 277, experimental lakes area, Northwestern Ontario, by addition of phosphate and nitrate. *Journal of the Fisheries Research Board of Canada*, 28: 1763-1782.
- Sotelo, J. L., Ovejero, G., Rodríguez, A., Álvarez, S. and García, J., 2013. Study of Natural Clay Adsorbent Sepiolite for the Removal of Caffeine from Aqueous Solutions.
- Srivastava V. C., Mall, I. D., and Mishra I. M., 2006. Characterization of mesoporous rice husk ash (RHA) and adsorption kinetics of metal ions from aqueous solution onto RHA, *Journal Hazard Materials*, 134: 257-267.
- Stratful, I., Brett, S., Scrimshaw, M.B. and Lester, J.N., 1999. Biological phosphorus removal, its role in phosphorus recycling. *Environmental Technology*, 20: 681-695.
- Strom, P.F., 2006. *Technologies to Remove Phosphorous from Wastewater*. Available at

- Suchi, S., and Meenakshi, C.S., 2009. Fluoride sorption using organic inorganic hybrid type ion exchangers, *Journal Colloid Interface Science*, 333: 58–62.
- Suzuki, T., 1990. Adsorption engineering, Kodansha, Tokyo, Japan.
- Tanjina, N., 2014. Nitrate, phosphate and fluoride removal from water using adsorption process. A Thesis submitted in fulfillment for the degree of Doctoral of Philosophy, University of Technology, Sydney.
- Theresa, M., 2002. Phosphate adsorption by mixed and reduced iron phases.
- Thi, A., Huu, H., Wenshan, G. and Tien Vinh Nguyen, 2012. Phosphorous Removal from Aqueous Solutions by Agricultural By products. *Journal of Water Sustainability*, 2: 193–207.
- Tillotson, S., 2006. Phosphate removal: an alternative to chemical dosing. *Filtration & Separation*. 43: 10-12.
- Tofik A.S. , Abi M. Taddesse, Tesfahun, K.T. and Girma G.G., 2016. Fe–Al binary oxide nanosorbent: Synthesis, characterization and phosphate sorption property. *Journal of Environmental Chemical Engineering*, 4: 2458–2468.
- Umar, M., 2011. Orthophosphate removal from domestic wastewater using limestone and granular activated carbon. *Desalination*. 271: 265 – 272.
- Vaclav S., 2000. Phosphorus in the environment: natural flows and human interferences. *annual review energy environment*, 25: 53–88.
- Van Loosdrecht, M.C.M., Hooijmans, C.M., Brdjanovic, D. and Heijnen, J.J., 1997. Biological phosphate removal processes. *Application Microbiol Biotechnolgy*, 48: 289–296.
- Weber ,W J. and Morris, J C, 1964. Kinetics of adsorption on Carbon from solution, *Journal Sanitary Engineeing Dvelopment*, 90: 79.
- WHO , 2002. Eutrophication and Health. Luxembourg.
- Worch, E. 2012. Adsorption Technology in Water Treatment: Fundamentals, Processes, and Modeling. Germany : Walter de Gruyter & Co.
- Xu, X., Gao, Y., Gao, B., Tan, X., Zhao, Y.-Q., Yue, Q. and Wang, Y., 2011. Characteristics of diethylenetriamine-crosslinked cotton stalk/wheat stalk and their biosorption capacities for phosphate'. *Journal of Hazardous Materials*, 192: 1690–1696.

- Xu, Y., Dai, Y., Zhou, J., Xu, Z.P., Qian, G., and Lu, G.Q.M., 2010a. Removal efficiency of arsenate and phosphate aqueous solution using layered double hydroxide materials. Intercalation vs. precipitation, *Journal of Materials Chemistry*, 20: 4684 – 4691.
- Yang, K., Yan, L., Yang, Y., Y, S., Shan, R., Yu, H., Zhu, B. and Du, B., 2014. Adsorptive removal of phosphate by Mg-Al and Zn-Al layered double hydroxides. Kinetics, isotherm and mechanism. *Separation and Purification Technology*, 124: 36-42.
- Yang, X., Xiao-lian, Z., Hao-ke, C., Kai-jie, L., Qi, L., and Dong-fang, L., 2013. Characteristics of phosphorus adsorption by sediment mineral matrices with different particle sizes. *Water Science and Engineering*, 6: 262-271.
- Yue, Q.Y., Wang, W.Y., Gao, B.Y., Xu, X., Zhang, J. and Li, Q., 2010. Phosphate Remova. from Aqueous Solution by Adsorption on Modified Giant Reed'. *Water Environment Research*, 82: 374–381.
- Zelalem Abebe, 2014. Study on phosphate removal capacity of water treatment residue (wtr) from wastewater adsorption process. Master Science in Environmental Science, Addis Ababa University.
- Zhang, L., Liu, J., Wan, L., Zhou, Q. and Wang, X., 2012. Batch and Fixed-Bed Column Performance of Phosphate Adsorption by Lanthanum-Doped Activated Carbon Fiber'. *Water, Air, & Soil Pollution*, 223: 5893–5902.

7. APPENDIX

Appendix 1. Calibration Curve

A calibration curve was prepared by using five known concentration of phosphate ions ranging from 5 mg/L to 15 mg/L. The calibration curve was plotted using the data from phosphate of known concentration and photometric absorbance reading (Table). The method utilized stannous chloride (APHA, 1998) to determine the concentration of phosphate ions. This method is based on the principle of ammonium molybdate reacts with phosphate ions and forms molybdophosphoric acid. This solution is reduced by stannous chloride forming blue complex which is directly proportional to the concentration of phosphate ions.

1. Experimental data used to prepare calibration curve from known concentration phosphate (independent) vs spectrophotometer absorbance reading (dependent)

| Sample solution with known PO ₄ ³⁻ concentration (mg/L) | STDEV | Mean absorbance reading |
|--|-------|----------------------------|
| 5 | 0.01 | 0.07 ± 0.01 |
| 7.5 | 0.02 | 0.12 ± 0.01 |
| 10 | 0.02 | 0.19 ± 0.02 |
| 12.5 | 0.01 | 0.26 ± 0.02 |
| 15 | 0.01 | 0.35 ± 0.01 |

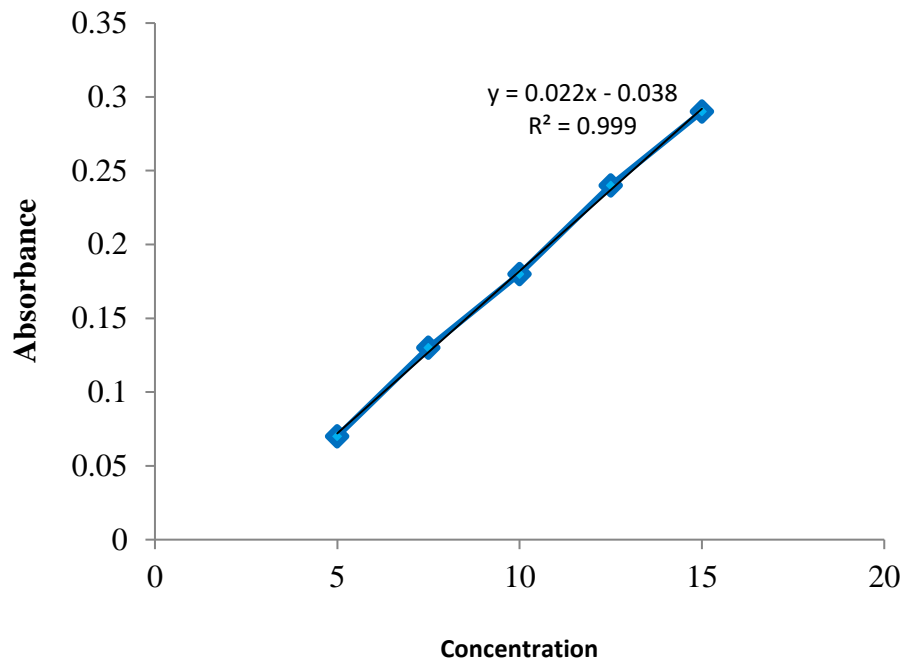


Figure 1. Calibration Curve prepared from Absorbance vs Concentration

The regression equation $Y=mX + b$ can be re-written as $X= (Y-b)/m$ so as to Calculate the residual phosphate concentration in the various batch adsorption test where:

“X” is Concentration of phosphate expressed in mg/L

“Y” is the photometric absorbance reading obtained from the spectrophotometer

“b” is the y-intercepts which was found out to be -0.0814

“m” is slope which was found out to be 0.0284

Appendix 2 . Data of adsorption parameters

Batch adsorption test experimental results used to calculate residual PO_4^{3-} concentration and adsorption capacity

2. Experimental Data Used to Analyze the Effect of pH on Phosphate Adsorption

| pH of sample solution | Adsorption efficiency (%) | Adsorption capacity (mg/g) | Mean residual phosphate concentration (mg/L). |
|-----------------------|---------------------------|----------------------------|---|
| 2 | 78.00 | 5.88 | 6.52 ± 0.02 |
| 3 | 81.99 | 6.15 | 5.61 ± 0.43 |
| 4 | 72.6 | 5.45 | 8.22 ± 0.04 |
| 7 | 71.8 | 5.39 | 8.45 ± 0.02 |
| 9 | 58.99 | 4.42 | 12.9 ± 0.02 |

3. Batch adsorption test results analyzed to determine the effect of ambo sandstone dose on phosphate adsorption

| Dose of Ambo sandstone (g) | Adsorption efficiency (%) | Mean adsorption capacity (mg/g) | Mean residual phosphate conc.(mg/L) |
|----------------------------|---------------------------|---------------------------------|-------------------------------------|
| 0.010 | 81.53 | 61.10 | 5.57 ± 0.02 |
| 0.050 | 83.37 | 12.59 | 4.82 ± 0.02 |
| 0.075 | 82.60 | 8.01 | 5.97 ± 0.01 |
| 0.100 | 82.10 | 6.19 | 5.24 ± 0.05 |
| 0.500 | 81.50 | 1.22 | 5.52 ± 0.06 |
| 1.000 | 78.50 | 0.55 | 8.16 ± 0.02 |

4. Batch adsorption test results analyzed to determine the effect of contact time on adsorption of phosphate by ambo sandstone

| Contact time (HRS) | Adsorption efficiency (%) | Mean adsorption capacity (mg/g) | Mean residual phosphate concentration (mg/L) |
|--------------------|---------------------------|---------------------------------|--|
| 3.0 | 74.72 | 12.10 | 5.8 ± 0.02 |
| 6.0 | 78.50 | 11.63 | 6.75 ± 0.04 |
| 12 | 80.80 | 11.69 | 6.62 ± 0.02 |
| 16 | 81.29 | 12.20 | 5.60 ± 0.04 |
| 24 | 81.1 | 11.22 | 7.56 ± 0.02 |

5. Batch adsorption test results analyzed to determine the effect of agitation speed on adsorption of phosphate by ambo sandstone

| Agitation speed (rpm) | Adsorption efficiency (%) | Mean spectrometer absorbance reading | Mean residual phosphate concentration (mg/L) |
|-----------------------|---------------------------|--------------------------------------|--|
| 50 | 81.29 | 0.078 ± 0.00 | 5.61 ± 0.01 |
| 100 | 79.29 | 0.095 ± 0.01 | 6.25 ± 0.02 |
| 120 | 84.30 | 0.052 ± 0.00 | 4.73 ± 0.02 |
| 140 | 80.43 | 0.085 ± 0.01 | 5.92 ± 0.02 |
| 160 | 79.77 | 0.091 ± 0.01 | 6.08 ± 0.02 |

6. Batch adsorption test results analyzed to determine the effect of initial concentration on adsorption of phosphate by ambo sandstone

| Initial concentration (mg/L) | Adsorption efficiency (%) | Adsorption capacity (%) | Mean residual phosphate concentration (mg/L) |
|------------------------------|---------------------------|-------------------------|--|
| 10 | 76.0 | 3.25 | 3.5 ± 0.01 |
| 20 | 65.0 | 5.12 | 9.91 ± 0.01 |
| 30 | 63.5 | 11.40 | 7.20 ± 0.05 |
| 50 | 51.0 | 12.75 | 24.50 ± 0.01 |
| 60 | 44.8 | 13.50 | 33.11 ± 0.02 |

7. Batch adsorption test results analyzed to determine the effect of co-existing ions on adsorption of phosphate by ambo sandstone

| Co-existing ions | Residual phosphate concentration (mg/L) | Adsorption efficiency (%) |
|--------------------|---|---------------------------|
| PO_4^{3-} | 7.37 | 85.0 |
| Cl^- | 6.32 | 87.4 |
| F^- | 4.59 | 90.8 |
| HCO_3^- | 6.98 | 86.1 |
| SO_4^{2-} | 6.388 | 87.0 |
| All | 6.10 | 87.8 |

8. Batch adsorption test results analyzed for determination of phzpc on adsorption of phosphate by ambo sandstone

| Initial pH | Final pH | Δ pH |
|------------|----------|-------------|
| 2 | 2.02 | 0.02 |
| 3 | 3.39 | 0.39 |
| 4 | 4.28 | 0.28 |
| 7 | 6.88 | -0.12 |
| 9 | 7.94 | -1.06 |

9. Batch adsorption test results analyzed for desorption of phosphate from ambo sandstone

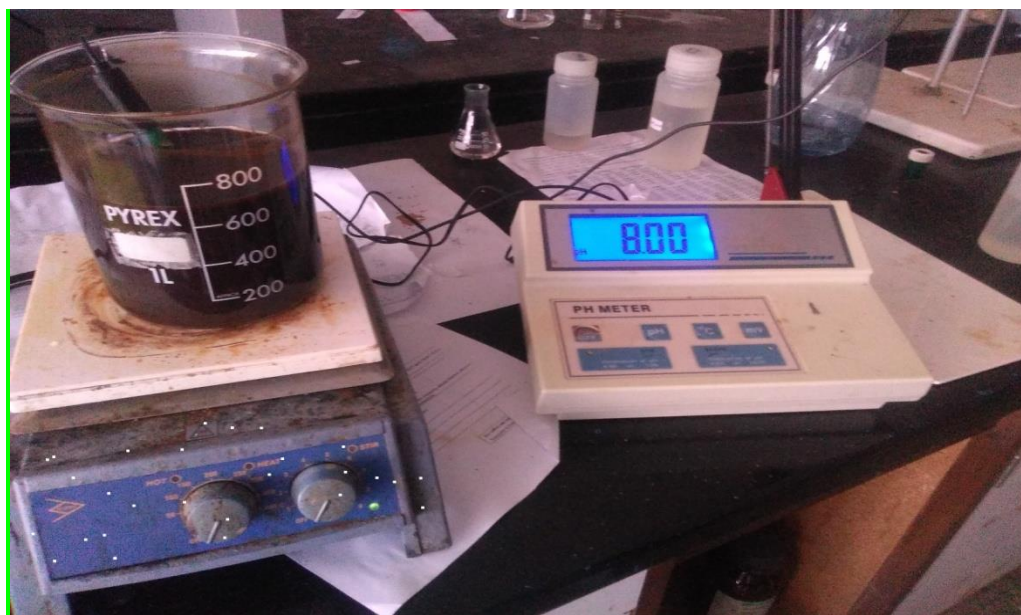
| pH | Amount of phosphate concentration (mg/L) | Desorption efficiency (%) |
|----|--|---------------------------|
| 2 | 8.75 | 20.00 |
| 3 | 6.88 | 18.90 |
| 4 | 8.96 | 20.71 |
| 7 | 9.06 | 20.94 |
| 9 | 9.59 | 22.00 |

Appendix 3 representative images depicting the various phosphate adsorption tests



Crushed Ambo sandstone before sieved

Crushed Ambo sandstone
after sieved



pH meter and hot plate



Preparation of residual phosphate through filtration for spectrometric determination



Rotary shaker for proper mixing of phosphate and sandstone



Color development during addition of reagent to residual phosphate